719934

ORNL-3492
UC-41 – Health and Safety
TID-4500 (22nd ed.)

Contract No. W-7405-eng-26

HEALTH PHYSICS DIVISION ANNUAL PROGRESS REPORT

For Period Ending June 30, 1963

K. Z. Morgan, Director
W. S. Snyder, Assistant Director
E. G. Struxness, Assistant Director

REPOSITORY MMES/X-10/Vault
COLLECTION Central File
BOX No. ORNL-3492
FOLDER

DATE ISSUED

SEP 23 1963

OAK RIDGE NATIONAL LABORATORY
Oak Ridge, Tennessee
operated by
UNION CARBIDE CORPORATION
for the
U. S. ATOMIC ENERGY COMMISSION

1147580

A-00383

Human Studies Project

Summary

PART I. RADIOACTIVE WASTE DISPOSAL

1. Liquid Injection into Deep Permeable Formations

The Ca-Sr exchange properties of numerous minerals show that these two cations behave quite similarly in ion exchange reactions. In cases where precipitation of slightly soluble salts occurs, the relative behavior may differ appreciably; strontium is less likely to be removed from solution than calcium by calcium carbonate but more likely to be removed by phosphatic minerals.

Solution dispersion due to formation heterogeneities is likely to lead to radionuclide dispersion a few orders of magnitude greater than that observed in laboratory columns. As a result, the factors affecting dispersion in laboratory columns are likely to be of little influence in affecting radionuclide dispersion in the environment.

In order to study geometric effects of dispersion of radionuclides by porous media and to test the effectiveness of physical and chemical barriers on a laboratory scale, a sandstone model has been constructed. The kinetics of ion exchange reactions observed in linear-flow columns will be extrapolated to the two-dimensional flow system, and the calculated response compared to measured values.

2. Disposal by Hydraulic Fracturing

An acceptable waste mix has been developed that is usable with waste solutions having a wide range of concentrations and chemical compositions. It is probable that an equally acceptable, cheaper mix can be developed that will require less of the expensive fluid-loss additive.

An injection and an observation well have been drilled, logged, cased, and cemented. These wells are 1080 ft deep; the main casing string of the injection well is $5\frac{1}{2}$ in. OD, and the main casing string of the observation well is $2\frac{7}{8}$ in. OD.

The design of the injection plant is virtually complete. The equipment consists of waste storage tanks, a waste transfer pump, four bulk storage tanks to store the solid constituents of the mix, a jet mixer, a high-pressure injection pump, and a standby injection pump and mixer. The mixer, injection pump, and wellhead valving will be installed in cells to reduce radiation exposure and limit the area of possible contamination.

In the proposed experiments several 40,000-gal batches of intermediate-level waste solution will be mixed with cement and injected into a shale formation at an approximate depth of 900 ft. At some time after the completion of the third injection the formation will be core drilled to verify the location of the grout sheets and to evaluate the various mixes.

3. Disposal in Natural Salt Formations

A 2-ft-high by 8-ft-wide model room was cut into a pillar to a depth of 10 ft, and closure rates were measured both before and during heating of the room to 160°C. The floor-to-ceiling closure rate after 40 days of heating (5×10^{-3} in./day) was two orders of magnitude higher than that at ambient temperature. Continued flow at this rate would completely close the room in 12 yr.

Measurements of creep closure in the Hutchinson, Kansas, mine in rooms ranging in age from about 1 to 27 yr indicate that closure rates decrease with age but increase with increased salt extraction. The floor-to-ceiling closure rates range from 8×10^{-4} to 1×10^{-4} in./day.

A demonstration of disposal of high-level radioactive waste solids is being designed for the Carey Salt Company mine in Lyons, Kansas. The

1147581

purposes of the demonstration are to perfect equipment and techniques and to investigate the synergistic effects of heat, radiation, and pressure on plastic flow, salt stability, and chlorine production. The demonstration will consist of a seven-can array of fuel assemblies, an electrical-heat-equivalent array, and two sets of electrical heaters to heat a pillar between the two arrays. Fourteen irradiated Engineering Test Reactor fuel assemblies will provide radiation in lieu of actual solidified waste. The test will last 2 yr; then all fuel assemblies will be returned to the Idaho Chemical Processing Plant for recovery of unfissioned fuel.

High-temperature studies on the disposal of high-level solid wastes have continued. In tests with 6-in.-diam by 4-ft-long heat sources (in 10-in.-diam by 10-ft-deep holes in the floor and wall), the effects of salt temperatures up to 350°C were investigated. Shattering of salt *in situ* in the Hutchinson mine occurred at about 280°C, in comparison to a range of 260 to 320°C determined from samples in the laboratory. Maximum reduction in hole diameter was 15%, due to nonrecoverable thermal expansion at a salt temperature of 350°C. Nonrecoverable expansion of about ½ in. of the floor and wall around the holes was also observed.

Experimental work on KCl has been used to calculate total production of chlorine in irradiated NaCl. After 200 days, a total of 0.5 mole of oxidizing agent would be produced per 6-in.-diam by 12-ft-long can of hypothetical (expected to be produced about 1975) solid waste. Irradiation of NaCl indicates that these values are conservative and that for short-term storage of high-level wastes in salt, little or no production of free chlorine can be expected.

Creep measurements in the Hutchinson mine indicate that the greater the percent of extraction, the greater the creep, and the older the age of the excavation, the lower the creep, with an average closure rate of 5×10^{-4} in./day.

Cores taken from the floor and roof of the Lyons mine showed that the only extensive pure salt deposits in the formation are those currently being mined. Therefore it was concluded that the experiment should be run in the same salt bed previously mined.

4. Clinch River Study

Results from the first year's water-sampling program indicate that most of the radioactive material entering the Clinch River from ORNL passes out of the river system in the water phase. The second year's data indicate some anomalous results, but thorough sampling of potential routes of contamination failed to reveal any other source than the monitored flow through White Oak Dam. Sampling has been discontinued until a new sampling program, designed to proportionally sample the flow releases from Melton Hill Dam, is installed.

Core samples from the Clinch River system were taken to obtain the radioactive material profile in the river and to determine the radioactive inventory in the bottom sediments. Specially designed counting equipment has been installed to automatically count the core in preset increments for gross gamma and to gamma-scan specific portions of the core.

Correlation analyses of the radionuclides in the bottom sediments indicate that Cs^{137}, Ru^{106}, TRE, and Co^{60} are apparently deposited by similar mechanisms and that Zr^{95}-Nb^{95} and Sr^{90} are deposited by different mechanisms. It may be possible to predict movement of the group of nuclides by counting just one.

Melton Hill Dam, a peaking power plant, will affect the hydraulic regime in the Clinch River by the sudden changes in discharge. Flume tests indicate that the effect of these changes will not cause greater dispersion than that observed with steady flow.

A preliminary safety analysis of the discharge of radionuclides to the Clinch River has been made. Dosages were compiled for the bone, gastrointestinal tract, thyroid, gonads, and total body for people at Clinch River Miles 14.5 and 2.6 and Tennessee River Miles 529.9 and 465.5, the critical points on the river system. For drinking water the largest fraction of $(MPC)_w$ attained was 0.51 in 1954. Variations in intake for sex and age differences indicate that dosages different than those obtained by standard man are possible. Immersion in contaminated water resulted in a maximum dose of 0.027 millirad/day in 1960. The greatest dose from bottom sediments was 12 millirads per day of exposure in 1959. Other potential sources of exposure being investigated are those due to ingestion of irrigated crops and contaminated fish.

1147582

5. Study of White Oak Creek Drainage Basin

Analyses of a series of 250 core samples taken in the bed of former White Oak Lake showed that, as of December 1962, the soil contained 1038 curies of Ru^{106}, 704 curies of Cs^{137}, 152 curies of Co^{60}, 17 curies of the rare earths (exclusive of Y^{90}), and 15 curies of Sr^{90}. Approximately 65% of the activity was found in the upper 6 in. of soil.

Studies on the movement of radionuclides in White Oak Creek indicate that (1) the amount of activity transported downstream by suspended solids is small during low creek flow rates and/or low suspended-solids loads, but during high stream flow and/or high suspended-solids loads, significant quantities of strontium and practically all the cesium are associated with sediments; (2) suspended solids of less than 9 μ sorb considerably more activity than larger particles; and (3) the amount of cesium associated with suspended solids increases considerably with a rise in the creek, and the amount of strontium associated with the liquid phase shows a pronounced increase.

Mean velocities in White Oak Creek of 0.4 to 2.3 fps at discharges ranging from 4.5 to 200 cfs have been determined from time-of-travel studies.

Water levels were measured in the permanent wells in White Oak Creek Basin in March (the time of highest ground-water surface) and showed greater annual variations at the higher elevations above the valley floor than at the lower elevations.

6. Mineral Exchange Studies

Heat-treated gibbsite is highly selective for strontium in alkaline systems. The capacity of heat-treated gibbsite is approximately 4 meq/100 g for cesium and 12 meq/100 g for strontium. The affinity for strontium of the heat-treated material is reflected by the lessened ability of sodium ions to desorb the strontium. After the sorbent was leached with sodium equal to 23 meq of Na^+ per meq of sorbed Cs^+, 96% of the cesium was desorbed; but when strontium was sorbed, only 77% of the strontium was desorbed after leaching with sodium equal to 730 times the amount of strontium on the sorbent.

Several other hydrous oxide minerals were heated to 500°C in order to determine whether this heat treatment could improve their properties for sorbing strontium. Goethite ($HFeO_2$), diaspore ($HAlO_2$), and limonite ($Fe_2O_3 \cdot xH_2O$) were used; heat-treated limonite showed the best strontium-sorbing characteristics.

Strontium removals by four different sorbents were compared using column techniques. Tests were performed using a 0.5 M $NaNO_3$ solution adjusted to pH 10 and containing 10^{-5} M $Sr(NO_3)_2$; the flow rate was 3 ml min^{-1} cm^{-2}. Commercial-grade activated alumina was most efficient; the 50% breakthrough volume for 10 g of material was approximately 6500 cm^3; the same weight of Dowex 50-X12 treated 2600 cm^3 for the same breakthrough percentage.

Sorption of trace quantities of cesium by vermiculite can be improved by pretreatment with potassium to increase the number of collapsed lattices available for edge fixation. Continued leaching of the treated vermiculite with 0.5 M $NaNO_3$, containing traces of cesium (1.7×10^{-7} M), releases the interlayer potassium and negates the pretreatment. Addition of potassium in the influent was found effective in maintaining potassium-treated vermiculite in a collapsed state. A concentration of 0.0005 M KNO_3 in 0.5 M $NaNO_3$ gave optimum cesium sorption (K_d = 366 ml/g) and a final exchange capacity of 46.8 meq/100 g compared to the initial exchange capacity of the potassium-saturated vermiculite of 5.9 meq/100 g.

Interlayer fixation of trace quantities of strontium was not observed when the vermiculite lattice was collapsed by addition of 0.01 to 0.04 M KNO_3 to 0.5 M $NaNO_3$ influent. The sorption of strontium was reduced by increases in the potassium concentration of the influent, and approximately 80% of the strontium was removed during the determination of the exchange capacity following column saturation.

7. Engineering, Economic, and Safety Evaluations

Studies of interim storage of calcined wastes and the effects of fission product removal on waste-management costs have been completed.

Interim storage facilities were designed to handle calcined waste cylinders for assumed storage periods of 1, 3, 10, and 30 yr. The computed costs of storage of Purex and Thorex wastes together in the same facility ranged from 0.0015 mill/kwhr (electrical) for 1 yr storage to 0.0048 mill/kwhr (electrical) for 30 yr storage for the

1147583

calcined acid wastes, and from 0.0018 to 0.0063 mill/kwhr (electrical) for the calcined reacidified wastes.

The object of the fission-product-removal study was to compare the waste-management costs for wastes with 90 and 99% of the fission products removed with the costs for managing the original waste with all fission products present. In each case, costs were estimated for the interim storage of liquid waste, pot calcination of waste, shipment of the calcined solids, and disposal of the solids in a salt mine. Total waste-management costs for the waste depleted of 99% of the fission products were only about 7% lower than for the 90%-depleted wastes, and both fell in the range of 0.017 to 0.019 mill/kwhr (electrical). Management costs for the original waste [0.024 mill/kwhr (electrical)] were only about one-third higher.

The tank storage hazard study has resumed under a modified set of basic postulates. Possible exposures of large populations to radiation resulting from accidental large-scale activity releases are being considered theoretically.

8. Related Cooperative Projects

The U.S. Geological Survey has continued to obtain partial-record base-flow and crest-stage records for the area. In addition, a geologic map of White Oak Creek Basin, with an explanatory text, has been prepared.

The multiagency steering committee for the Clinch River Study has continued.

Three alien guests have been on assignment during the past year.

Several members of the Section have continued to participate in the following activities: the ASA Committee N5, the AEC Advisory Committee on Deep-Well Disposal, the ASCE Committee on Sanitary Engineering Aspects of Nuclear Energy, and various ORNL special committees; members have also contributed to the journal *Nuclear Safety*.

In addition, courses and lectures have been given for ORSORT, Vanderbilt University, and the U.S. Public Health Service.

PART II. RADIATION ECOLOGY

9. Radioactive Waste Area and Radiation Effects Studies

In new dosimetry studies, miniature metaphosphate glass rods are being used to estimate absorbed dose in air and in the plants and soils of White Oak Lake bed. Combined beta and gamma doses in the top inch of mineral soil ranged from 20 to 25 rads/day on the northwest edge of the lake bed where Ru^{106} seepage from higher ground is appreciable. Absorbed doses in air at the surface of marsh plants (*Typha latifolia* L.) in this area ranged vertically from 6.2 rads/day at ground level to 2.8 rads/day at 5 ft above the ground. Absorbed doses in stem tissue of these plants were 23% higher due to absorbed radionuclides, principally Ru^{106}. The dose to root systems was three to seven times higher than the dose to shoot components.

In food-chain studies of cotton rats maintained in pens on White Oak Lake bed and feeding on native vegetation, it was found that (1) the concentrations of radionuclides in tissues are positively correlated with the corresponding concentrations in stomach contents and plants, (2) the concentrations of radionuclides in tissues are not correlated with corresponding concentrations in soil, (3) Sr^{90} in femurs is the only radionuclide in the tissues which was in greater concentration than in food or plants, and (4) the placental and mammary barriers apparently were effective in reducing the concentration of Sr^{90} in fetuses and nursing young.

Blood samples were taken from the original cotton rats one week before release into pens and at 4- to 6-week intervals thereafter. Blood analyses were also made on samples from rats born in the pens. Analyses of erythrocyte and leucocyte counts, leucocyte differential counts, hematocrits, mean corpuscular volumes, cell-volume distributions, and total serum solids were performed. These analyses showed no apparent effects of ionizing radiation in the blood of cotton rats maintained in the pens for this first experiment.

Studies on hematology of native mammals continued to support the discovery last year that the number of erythrocytes is inversely related to species size and that the mean erythrocyte volume is directly related to the species size. This

1147584

relation was found to be present in the rodent families Muridae and Sciuridae, the shrew family Soricidae, and the primate family Cebidae. Seasonal effects on the blood of native mammals are being followed because of variations noted in cell counts and hematocrits of the blood of mammals trapped during various seasons of last year. Erythrocyte counts and hematocrits, for instance, in some species seem to be higher in the winter than during other seasons.

Use of trees as long-term monitors of radioactive seepage from underground waste pits was tested by sampling even-age pines growing around waste pit No. 5. Significant concentrations of four gamma-emitting radionuclides were found in these pine trees. These nuclides were Ru^{106}, Zr^{95}-Nb^{95}, Cs^{137}, and Ce^{144}. Concentration of Ce^{144} was between 100 and 200 $\mu\mu c$ per g of dry weight, which is the same as fallout levels. Cesium-137 concentration was uniform in all trees at 30 to 70 $\mu\mu c$ per g of dry weight. This amount could be attributed to blowout from three open pits which are due west of waste pit No. 5. Ruthenium-106 concentration varied from 0.02 μc per g of dry weight to fallout levels, which are 40 to 70 $\mu\mu c$ per g of dry weight. Twenty-three of the seventy-three trees collected showed a concentration of Ru^{106} greater than that which could be attributed to fallout or to blowout from the open pits. This higher concentration is attributed to seepage (and subsequent uptake by the tree) from waste pit No. 5. Five trees showed a concentration of Zr^{95}-Nb^{95} which was greater than fallout levels and also greater than Ru^{106} levels. The highest concentration of Zr^{95}-Nb^{95} was 771 $\mu\mu c$ per g of dry weight. Concentration of all the isotopes except Zr^{95}-Nb^{95} tended to be greater in needle material than in twig material.

Fission foil threshold detectors were used to determine the fast-neutron dose absorbed by white oak acorns irradiated in the ORNL Graphite Reactor. The acorns were irradiated in a 17 × 8 × 4.5 in. box of boron carbide–impregnated Lucite, which absorbed thermal neutrons (over 50% of the total flux) but allowed fast neutrons to pass through the seed. Fission foils and pellets of S^{32} were placed under and on top of the sample to be irradiated – seed stacked to a depth of 4 in. After irradiation the foils and sulfur were counted immediately in the special fission foil counters of the Health Physics Division. Dose calculations were made according to the method of Hurst and Ritchie. The dose under 4 in. of acorns was 1755.8 rads/hr, whereas the dose over 4 in. was approximately 1250 rads/hr.

Use of biological elimination of radioisotopes in insects as indirect measures of metabolism under field conditions was continued with emphasis on the influence of temperature on elimination rates. In geometrid caterpillars the biological half-life of Cs^{137} was decreased by one-half for a 10° rise in temperature. Similar temperature-related trends were found for leaf beetles (*Chrysomela knabi*) and millipedes (*Dixidesmus erasus*).

10. Forest Studies

Computer feedback models have included compartments for woody materials, as a step toward interpreting patterns of forest growth. The positive feedback representing increased photosynthetic rate with increased foliage mass is counteracted by opposing negative feedbacks, representing not only the loss rates from respiration and other processes (litter fall, consumption, translocation) but also a "limiting feedback" related to the capabilities of an area for producing organic matter. Diurnal and seasonal cycles of production have been combined in the same model.

Further analyses of two- and three-year comparative experiments, in cooperation with the Botany Department of the University of Tennessee, showed different rates of breakdown for several kinds of deciduous leaves measured in the Oak Ridge Reservation and the Great Smoky Mountains. In all environments, leaf species showed large and consistent differences in weight loss of leaves confined in bags of nylon net. Mulberry decayed rapidly to black humus, losing 0.002 to 0.0046 of its total weight per day in different environments. Beech showed the slowest visible signs of decay, with fractional weight losses of only 0.0003 to 0.0012 per day. White oak, Shumard red oak, and sugar maple showed intermediate rates of weight loss and visible destruction. Yearly differences in decay rates emphasize the need for several-year experiments, using closely compared sets of techniques, for drawing generalizations about rates of ecological processes which affect the movement of nutrients or isotopes in contrasting environments.

Seasonal measurements of microbial populations of four leaf species in three contrasting forest

1147585

types during the first year showed a highly significant correlation between leaf weight loss and microbial respiration, especially that of bacteria. Seasonal fluctuations of microbial respiration were primarily correlated with temperature, but other significant correlations were found with bacterial counts, moisture content of the leaves, and age of the litter.

The first large-scale tracer experiment employing Cs^{137} in a small stand of yellow poplar is confirming the expectation of rapid circulation of Cs^{137} through the forest ecosystem. The rapid attainment of maximum foliage concentrations in June was followed by a decrease throughout the growing season. Evidence was found of a marked withdrawal of Cs^{137} from the leaves back into the trunk prior to leaf fall. Rainwater collections further supported the possibility that in late summer there is a period in which alkali metal reserves are remobilized into the tree. Paper chromatography analyses, autoradiograms, and column elution tests showed that the bulk of Cs^{137} activity is in the phloem tissue (parenchyma), where it exists only in the ionic form, and that only ionic bonding takes place between the cesium and the wood.

In addition to Cs^{137} income from rainfall and litter fall, downward movement of Cs^{137} in roots of tulip poplar apparently provides an important contribution of this nuclide into the soil (Emory silt loam) of the tagged forest. Early litter sampling on lines on a close spacing (2 cm) showed very abrupt variation, due partly to uneven movement of rainout over the incomplete litter cover of the mull humus. The extent of variation within centimeter distances was greater than two orders of magnitude. Early sampling indicated the importance of root contribution to the highly variable initial distribution. Root fragments which could be separated from inorganic soil particles contributed at least 90% of the total activity as of July 16, 1962. Fine rootlets that could not be separated from sieved mineral soil may already have contributed to radioactivity in this and subsequent samples.

Wide differences in concentrations of Cs^{137} were found in mushrooms growing on the tagged forest floor. This variability was not only the result of large differences among substrates but also the result of differences within one substrate at different locations. Concentrations of Cs^{137} in litter were from 0.1 to 68 times lower than the concentrations in the underlying soil and roots. Variations in concentrations of Cs^{137} in mineral soil exceeded two orders of magnitude for surface samples taken only 10 cm apart.

Two types of food chains are being compared in the tagged forest: the green foliage–herbivorous arthropod–predaceous arthropod type of food chain and the leaf litter–herbivorous arthropod–predaceous arthropod type. Cesium-137 concentrations were lower in the leaf litter–soil arthropod food chain than in the green foliage food chain, since leaching of cesium from green leaves was the radioisotope source for the litter layers. Radioisotope concentration in leaf litter increased gradually during the summer and abruptly during the early autumn as leaf fall progressed. During the summer months herbivores had Cs^{137} concentrations almost as high as the concentration in leaf litter. Herbivore radioactivity increased in the autumn but not as rapidly as did leaf litter radioactivity. Predators also showed an increase in Cs^{137} content during the summer and early autumn. During July and August the herbivore and predator parts of the leaf litter–soil arthropod food chain had an added input due to direct feeding on the green foliage. Phalangids (*Liobunum* sp.), for example, had Cs^{137} contents which were a factor of 2 or more higher than leaf litter concentrations. Also, some of the predators were evidently feeding in the green foliage food chain although they were trapped on the forest floor. The result was that the animal portions of the leaf litter food chain appeared abnormally high during July and August. In October the green foliage had disappeared, and the leaf litter food chain assumed a Cs^{137} distribution resembling that of the green foliage food chain.

11. Clinch River and Related Aquatic Studies

Aquatic studies continue to emphasize the fate and effects of radionuclides released to the Clinch River via White Oak Creek. Analyses of stable strontium in the flesh and bone of white crappie were continued to test the relation of the distribution of stable strontium and Sr^{90} between the environment and the fish. If the distribution of stable strontium and Sr^{90} between fish tissue and water are the same, it should be possible to predict Sr^{90} concentrations in tissue for continuous environmental releases. Samples have been taken

1147586

at monthly intervals to determine whether there are seasonal changes in the strontium concentrations in fish tissue. The average stable-strontium concentration in bone is 271 ± 6.34 ppm (± one standard error) based on 105 samples. This quantity of strontium in bone is a concentration factor of 4.0×10^3 over that in Clinch River water. Strontium concentrations in flesh average 0.0813 ± 0.0118 ppm (27 samples), which is a concentration factor of 1.2 over that of river water.

The biological half-life of strontium in white crappie has been determined by tagging fish with Sr^{85} and then counting the same fish at 1-min intervals in a small-animal whole-body counter. In experiments completed, the biological half-life of strontium in the flesh of different individuals has ranged from 12 to 48 min, somewhat shorter than anticipated previously. Measurement of the turnover of strontium in flesh was complicated by the rapid deposition and high concentration of strontium in fish bone, which literally masked the strontium in soft tissues. This difficulty was circumvented by constructing a fish-holding assembly and inserting it in the detector chamber of the counter. Water was pumped through the assembly during the experiments to remove excreted Sr^{85} and to provide a supply of oxygenated water.

The transport of Sr^{90} from the Clinch River by emerging aquatic midges (Chironomidae) was compared with the accrual of Sr^{90} to the river from weapons-testing fallout. Larval development of the midges occurs in the contaminated river-bottom sediments. Emerging adults were caught in insect light traps operated on the river bank at dusk. Adults in one large, composite sample contained 8.76 times as much Sr^{90} [$(3.55 \pm 1.13) \times 10^{-6}$ μc per gram of dry weight] as did an equal quantity of river-bottom sediment from the same location. Studies elsewhere have shown that 10 g m^{-2} yr^{-1} may be contained in the emergent insect biomass. These emergent insects would transport $(3.55 \pm 1.13) \times 10^{-5}$ μc of Sr^{90} per square meter per year from the river bottom. The average increment of Sr^{90} from fallout in the United States between 1959 and 1960 was 4.2×10^{-3} curie/square mile (1.62×10^{-3} $\mu c/m^2$). Thus, fallout entering the river directly would add 45 times as much Sr^{90} as removed by emerging chironomids.

Studies of the relative influence of stable strontium and stable calcium on strontium are in progress using the snail *Physa heterostropha* and highly purified and assayed calcium carbonate. Preliminary results suggest that strontium uptake is dependent primarily on stable strontium in the environment.

A study of the age distribution, growth rates, and dispersion of smallmouth buffalo, *Ictiobus bubalus* (Rafinesque), in Watts Bar Reservoir, and of their importance as an accumulator of radionuclides, was completed. The ages of 1271 commercially caught fish ranged from 4 to 15 yr; the largest number were from year class 6, the youngest year class which was completely vulnerable to commercial fishing gear. Total survival rates were found to be 49% for year class 6, 35% for year class 7, 26% for year class 8, and 19% for year class 9.

A high concentration of radionuclides in the environment was found to be necessary for smallmouth buffalo to accumulate measurable quantities in their scales. White Oak Creek is the only area of Watts Bar with sufficient radionuclide contamination for such accumulation to occur. If surface area is considered a measure of available fish habitat, White Oak Creek comprises less than 0.02% of Watts Bar Reservoir at full pool. Only a small percentage of the population would be expected to be resident in the contaminated area. However, with mobile populations contamination could be expected in larger numbers of fish because of movement into and out of White Oak Creek. This contamination could be detected in tissues such as bone or scales having a long biological half-life for the several radionuclides released. Radiometric surveys of scales revealed the smallmouth buffalo population of Watts Bar Reservoir to be a relatively minor accumulator of radionuclides, with only 0.08% having a detectable accumulation in their scales. Approximately 6% of the Clinch River fish and 77% of the White Oak Creek fish had measurable radionuclide accumulations.

The salivary gland chromosomes of *Chironomus tentans* larvae collected from White Oak Creek, an area contaminated by radioactive waste from ORNL, and from six uncontaminated areas were examined for chromosomal aberrations. White Oak Creek populations were exposed to a dose rate calculated as 230 rads/yr, or about 1000 times background. Fifteen different chromosomal aberrations were found in 365 larvae taken from the irradiated population as compared with five different aberrations observed in 356 larvae from six

1147587

control populations, but the mean number of aberrations per larva did not differ in any of the populations. The quantitative amount of heterozygosity was essentially the same in the irradiated and the control population, but there was three times the variety of chromosomal aberrations found in the irradiated area. From this evidence it was concluded that chronic low-level irradiation from radioactive waste was increasing the variability of chromosomal aberrations without significantly increasing the frequency.

PART III. RADIATION PHYSICS AND DOSIMETRY

12. Theoretical Radiation Physics

Calculations of rad and rem doses in a tissue slab from protons with energies up to 400 Mev have been completed. A code has also been developed for calculating dose in a finite geometry phantom (parallelepiped), and results for this case are nearing completion. Preliminary studies at proton energies greater than 400 Mev are in progress.

A code has been written to compute the distribution of dose with LET, in order to analyze the biological response of animals exposed to neutron irradiation. An investigation of shell corrections in atomic stopping-power theory has been made. The low-energy end of the slowing-down spectrum of electrons in a free-electron gas has been computed using a numerical solution of the appropriate integral equation and numerical values of the requisite interaction cross sections. The dispersion relation for surface plasmons has been investigated in a semiclassical approximation. An analytic solution for the distribution of transition radiation from a two-layered foil has been obtained. A semiclassical derivation has been given of the cross section for photon absorption in metals due to the presence of impurity scattering centers. A formulation of the constitutive equations for a moving medium has been given. The interaction of an electron or an ion beam moving through a stationary plasma has been investigated.

13. Experimental Physics of Dosimetry

Recent work on the interaction of alpha particles with water molecules reveals that the interaction is a physical process in which the cross section for momentum transfer is a factor of 2 larger than that obtained from theory. The cross section for the dissociative electron capture process in D_2O has been measured and compared with that obtained in H_2O.

The recently developed time-of-flight technique for investigation of electron transport in gases has been applied to the measurement of drift velocities and diffusion coefficients in several gases and, in particular, in mixtures of water vapor and ethylene. A newer version of the electron time-of-flight machine is under construction and will permit measurements to be made for a wider range of gases. A combination of spectroscopic and ionization experiments on the effect of alpha particles on atomic argon has led to a rather complete description of the ways in which alpha particles interact with atomic argon.

The angular and spectral distribution of photons emitted by silver foils, 660 and 1980 A thick, when bombarded by 40-kev electrons has been determined experimentally in the wavelength region 2500 to 5600 A. The spectral distribution of light polarized in the plane of incidence showed a sharp peak at 3300 ± 12 A, this value being an average over photon directions 10 to 50° from the foil normal. In addition to the peak, the spectrum showed a continuum which decreased slowly with increasing wavelength and a deep minimum at 3200 A with a rise in the shorter wavelengths. The angular distribution of photons emitted at the peak wavelength showed a maximum at 30° from the foil normal with zero intensity at 0° and near 90°, whereas the photons emitted at other wavelengths in the continuum, for example, at 2700 and 4500 A, were most intense at 50° from the foil normal.

An operational analyzer has been designed and built for generalized dosimetry applications.

The transmission, resolution, and energy calibration of the Keplertron, a spherical electrostatic analyzer, have been further checked with the Sm^{152} Auger line at 32.8 kev and the Ni^{64} Auger line at 6 kev from relatively thin sources of Eu^{152} and Cu^{64}, respectively, and found to be in good agreement with the values previously determined at lower energies by means of an electron gun. The electron slowing-down spectrum in copper of negatrons from Cu^{64} has been measured with the Keplertron and found to be in absolute agreement from 37 kev to 1 kev with the Spencer-Fano theory. Difficulties in experimental techniques used in

1147588

making the above measurement have either been corrected or are under study. Programs have been written for the CDC 1604 computer to calculate theoretical spectra and to correct experimental data.

14. Physics of Tissue Damage

The intensity of thermoluminescence has been shown to depend strongly upon the presence of a gas both during the irradiation of the sample and during the subsequent warmup. Experiments have been conducted in an effort to understand the mechanisms involved in this gas effect. One experiment was an attempt to observe whether the ions or electrons formed in the gas during irradiation influenced the thermoluminescent intensity. This experiment gave negative results. An attempt was also made to detect by gas chromatography gaseous emissions from the samples, particularly as these might correlate with the optical emissions. A more sensitive experiment along these lines is now being conducted. A third experiment involved the technique of electron spin resonance. Correlations between the numbers of radiation-induced spins and integrated thermoluminescent intensity for varying sample crystallinities and gaseous conditions were sought. No gaseous dependence of spin resonance signals was found.

An electron gun is under development which will permit studies of electronic energy levels excited in solids and gases by the passage of fast electrons. A time-of-flight energy selection will be used to obtain an electron beam homogeneous in energy to 0.01 ev, thus enabling studies of energy levels of this or higher energies. The gun, drift tube, and electronics have been assembled, and bursts of electrons having energies between 2 ev and 15 ev have been obtained. The square of the reciprocal arrival time was found to be a linear function of the electron energy as expected from elementary kinematics. A new gun, ultrahigh vacuum system, and open-window electron multiplier are being installed so that studies of beam gating by electrostatic and magnetic methods may be made.

15. Radiation Dosimetry

The major effort of the Radiation Dosimetry Group was directed to the Ichiban Dosimetry Program, dosimetry research, and installation of the Health Physics Research Reactor. Analysis of most of the data from Operation BREN was completed, and the HPRR commenced routine operation on May 31, 1963. A study was completed on the long-term buildup and fading in metaphosphate glass.

PART IV. INTERNAL DOSIMETRY

16. Estimation of Internal Dose

The program of the Internal Dose Estimation Section is directed toward radioactive materials which enter the body. In particular the maximum concentrations are estimated for radioactive materials in air, $(MPC)_a$, or in water, $(MPC)_w$, that would limit the burden to a prescribed amount over a working life.

A retention function has been defined which represents the retention of strontium in the body over extended periods of adult life. The function consists of three exponential terms, two of which are obtained by simultaneously adjusting the parameters so that retention and excretion data during the period of about 100 to 200 days following injection of strontium are represented. The third exponential is obtained by selecting parameters to make the function consistent with data on levels of stable strontium in diet and in bone of Western man and to be in fair agreement with data on the rate of remodeling of bone. Thus the function is in reasonably good agreement with the data now available on chronic retention of strontium in normal adults. Using this model, $(MPC)_w$ values for Sr^{90}, Sr^{89}, and Sr^{85} are obtained and compared with values derived on the basis of other models. On the basis of the general agreement of these models, it is suggested that an $(MPC)_w$ of 4×10^{-6} $\mu c/cm^3$ is acceptable for occupational exposure (168 hr/week) to Sr^{90}.

17. Stable-Element Metabolism by Man

The elemental composition of bodies of grossly normal adults provides one of the best sources of information concerning the distributions of various isotopes within the body that are to be expected following chronic exposure to the materials. In the search to determine the elemental composition of standard man, 415 bone samples were analyzed from long-term residents of 11 major cities in the

1147589

United States and 13 cities in foreign countries. Each sample was examined for 20 elements. These data are perhaps the most extensive source of information on the concentrations of many trace elements in bone.

The accuracy of the Quantometer values was checked for several elements using atomic absorption, flame spectrophotometry, and colorimetry. In each case the agreement was generally good.

The influence of age, race, and geographical location on the trace-element content in tissue has been studied. On the whole the concentrations of trace elements were not different from those in adults, but certain elements showed significant variations. Except for the higher lead ($p \leq 0.05$) in kidney, liver, and lungs of males, there were no sex differences in the American group. There appeared to be no significant differences due to race *per se*.

PART V. HEALTH PHYSICS TECHNOLOGY

18. Aerosol Physics

Fundamental and engineering studies of radioactive surface contamination are continuing. Major emphasis is on the development of reproducible sampling techniques for evaluating the extent of particulate contamination on surfaces and the application of redispersion test results to the establishment of contamination control criteria. Studies of contamination sampling indicate that the smear and adhesive paper methods are strongly affected by the characteristics of the surface, the concentration of the contaminant, and variations in technique among monitoring personnel. A new sampling method, employing air dispersion, is essentially independent of surface roughness and dustiness, and results in minimal monitoring variation among different personnel; redispersion efficiency varies with particle size of the contaminant and with velocity of the air impinging on the surface.

The adsorption of radioactive iodine vapor onto condensation nuclei has been investigated by use of aerosols produced by exploding silver and platinum wires. In the absence of aerosol particulates, the iodine vapor diffuses to the container walls with a half-life of 49 min. When the metallic aerosols are mixed with the iodine vapor, iodine concentration in the container is lost at a much slower rate. In the case of platinum aerosol, 17% of the iodine is associated with a particulate phase which is lost to the container walls with a half-life of 6.9 hr; the remainder is lost with a half-life of 41 min. The silver aerosol adsorbs and retains the iodine much more effectively than does the platinum aerosol.

The high-volume annular impactor is an air sampling device which employs inertial forces to deposit airborne particulates on a collecting surface. Dust deposition patterns usually include a central circular deposit and one or more annuli of deposited dust with definite minima or clear areas separating the deposition sites. Study of the design and operating parameters of the device has shown that deposition of dust at the center and at the primary impaction annulus begins as soon as the sampler is started; all parts of the pattern develop concurrently. Investigation of the airflow patterns near the collecting surface indicates the presence of at least two stable, toroidal vortices contiguous to the surface. To a considerable degree, the patterns of static pressure distribution and dust deposition appear to be correlated.

Tests have continued to explore the capabilities of the exploding wire aerosol generator to produce and disperse a wide variety of submicron aerosols. Aerosols can be produced which differ greatly in chemical composition, density, electrical and thermal conductivity, permittivity, and other physical properties which may be of interest in testing instruments or simulating health physics field problems in the laboratory. Wires or foils of 18 different metals have been exploded in a nitrogen atmosphere. The pertinent data regarding yield and composition of the resultant aerosols are tabulated. It was found that aerosol yield increases with increasing gas pressure in the explosion chamber at all operating voltages, but the primary particle size is not affected dramatically by either pressure or voltage. These and other findings of the study may indicate that particle formation in the exploding wire phenomenon occurs in the shock wave.

19. Applied Internal Dosimetry

Continuing improvements of instrumentation and operating program at the ORNL In Vivo Gamma-Ray Spectrometry Facility (IVGS) have made it possible to increase the rate of routine in vivo counts for monitoring purposes and, at the same time, initiate

1147590

17%
iate
with
th a
and
than

air
rces
cting
clude
nuli

a limited research program. A thin-crystal assembly [three NaI(Tl) crystals 5 in. in diam by $^{1}/_{16}$ in. thick] is now available for use in the spectral analysis of electromagnetic radiation in the energy region below 150 kev. Thin crystals are particularly important in the study of lung burdens of plutonium. At present, the assembly can detect slightly less than 40 nanocuries of Pu^{238} in the chest region, provided a background count is made on the individual prior to the plutonium exposure (four standard deviations). If no such prior count is available, the limit of detection is increased to

subjects also submitted total voiding urine during the study. The amounts of I^{131} ingested were small in comparison with permissible levels but provided adequate counting rates. Two cases of single ingestion and three cases of repeated daily ingestion were compared. Best-fitting curve plots of the data were obtained by the least-squares method using two different weighting factors. The data, presented in tables and graphs, show that extrapolations from single intake data and the application of ICRP-NCRP parameters provided slight overestimates of the thyroid and whole-body

completed the program at Vanderbilt University and Oak Ridge, and the Fellowship group for the 1963–64 program has been selected. Lectures and laboratory courses were provided for laboratory, division, and civic programs.

It is anticipated that in the future more training in health physics will be provided for ORNL personnel and for foreign students on an individual basis.

1147592

ıining
)RNL
·ıdual

Contents

SUMMARY iii

PART I. RADIOACTIVE WASTE DISPOSAL

1. LIQUID INJECTION INTO DEEP PERMEABLE FORMATIONS 3
   - Strontium Exchange by Sandstones 3
   - Fission Product Dispersion in the Ground 6
   - Radionuclide Migration and Dispersion in Sandstone 7
2. DISPOSAL BY HYDRAULIC FRACTURING 13
   - Mix Development 13
   - Well Drilling 15
   - Plant Design 16
3. DISPOSAL IN NATURAL SALT FORMATIONS 19
   - Heated Model Room 19
   - Demonstration of High-Level Waste Solids Disposal in Salt 22
   - High-Temperature Experiments 29
   - Chlorine Release from Gamma-Irradiated Salt 32
   - Creep Measurements in Mines 34
   - Floor and Ceiling Cores 35
4. CLINCH RIVER STUDY 37
   - Water Sampling and Analysis 37
   - Bottom Sediment Studies 38
   - Hydrology 44
   - Safety Analysis 45
5. STUDY OF WHITE OAK CREEK DRAINAGE BASIN 51
   - Quantity, Distribution, and Transport of Radionuclides in the Bed of Former White Oak Lake 51
   - Movement of Radionuclides in White Oak Creek 57
   - Time of Water Travel in White Oak Creek 60
   - Ground-Water Levels in White Oak Creek Basin 60
6. MINERAL EXCHANGE STUDIES 62
   - Strontium Removals by Hydrous and Anhydrous Sesquioxides 62
   - Strontium and Cesium Removal by Vermiculite 67

1147593

7. ENGINEERING, ECONOMIC, AND SAFETY EVALUATIONS 70
Engineering and Economic Evaluations 70
Interim Storage of Solidified Wastes 71
Effects of Fission Product Removal 72
Tank Hazard Study 73
Activity Distribution 73
Atmospheric Dispersion 74

8. RELATED COOPERATIVE PROJECTS 76
Geologic and Hydrologic Studies by U.S. Geological Survey 76
Cooperation of Other Agencies in ORNL Studies 77
Visiting Investigators from Abroad 77
Nuclear Safety Review 77
Committee Work 78
Participation in Educational Programs 78

PART II. RADIATION ECOLOGY

9. RADIOACTIVE WASTE AREA AND RADIATION EFFECTS STUDIES 81
Glass-Rod Dosimetry in Environmental Studies 81
Penned-Mammal Study 81
Hematology of Native Mammals 88
Use of Radioactive Tags to Evaluate Movements of Wild Mammals 88
Distribution of Gamma-Emitting Nuclides in Trees Bordering Radioactive Waste Pit No. 5 89
Vegetation Studies Around the HPRR 92
Neutron Dosimetry and Seed Irradiation 92
Gamma-Ray Dosimetry in Cs^{137}-Tagged Tulip Poplar 93
Use of Radioactive Tracers for Analysis of Food Chains 94

10. FOREST STUDIES 95
Computer Feedback Models 95
Components of Forest Litter Fall 96
Rates of Litter Breakdown in Contrasting Climates 97
Transfer of Co^{60} and Ru^{106} from Oak and Ash Leaves to Several Forest Soils 97
Microbiology of Forest Litter 98
Gross Effects of Arthropods and Microflora on Rates of Leaf Litter Breakdown 98
Leaf Litter Consumption by Millipedes 100
First-Season Redistribution of Cs^{137} in Canopy of a Tagged *Liriodendron* Forest 100
Determination of Potential Cesium-Organic Binding Sites in *Liriodendron* and Other Woody Species 102
Entry of Cs^{137} into Litter and Soil of a Tagged *Liriodendron* Forest 104
Microbial Immobilization of Radionuclides in Forest Litter 105
Mobility of Cs^{137} in Forest Food Chains 106

1147594

70 11. CLINCH RIVER AND RELATED AQUATIC STUDIES 107
70 Strontium in White Crappie (*Pomoxis annularis*) Flesh and Bone 107
71 Biological Movement and Reservoirs of Sr^{90} 109
72 Uptake and Accumulation of Strontium by Algae and Snails 109
73 Smallmouth Buffalo Population Studies and Fish Marking 110
73 Population Genetics and Radiation Effects Studies on *Chironomus tentans* 112
74 Safety Evaluation of Clinch River Fisheries 114
76 Related Activities 115
76
77 PART III. RADIATION PHYSICS AND DOSIMETRY
77 12. THEORETICAL RADIATION PHYSICS 119
77 Dosimetry of High-Energy Protons 119
78 Studies Concerning the Relation of RBE and LET 123
78 Shell Corrections to Atomic Stopping Power 124
Low-Energy End of the Secondary Electron Cascade in Metals 125
Surface Plasmon Dispersion Relation 127
81 Transition Radiation from a Two-Layered Foil 128
81 Photon Absorption in Metals Due to Impurity Scattering Centers 129
81 Constitutive Equations for a Moving Medium 130
88 Instabilities in a Plasma-Beam System Immersed in a Magnetic Field 131
88 13. EXPERIMENTAL PHYSICS OF DOSIMETRY 134
89 Electron Interactions with Water Molecules 134
92 Time-of-Flight Investigations of Electron Transport in Gases 135
92 Interaction of Energetic Charged Particles with Atomic Argon 137
93 Measurement of Transition Radiation and Optical Bremsstrahlung from Electron-Bombarded Metal Foils 137
94 Spherical Electrostatic Analyzer and Electron Slowing-Down Spectra in Copper 141
95 An Operational Analyzer for Generalized Dosimetry 142
95 14. PHYSICS OF TISSUE DAMAGE 143
96 Effects of Adsorbed Gas on Optical Emissions of Irradiated Biochemicals 143
97 Time-of-Flight Electron Beam Monochromator 144
97 15. RADIATION DOSIMETRY 146
98 Gamma-Ray Spectrometry 146
98 Fast-Neutron Spectrometry 146
100 Gamma-Ray and Fast-Neutron Dose as a Function of Incidence Angle 147
100 Energy Response of BREN Normalizing Counter 150
Spatial Dose Distribution in Air-over-Ground Geometry 151
102 Radiation Measurements over Simulated Plane Sources 152
104 Metaphosphate Glass Microdosimeters 153
105 Health Physics Research Reactor (HPRR) 154
106

1147595

PART IV. INTERNAL DOSIMETRY

16. ESTIMATION OF INTERNAL DOSE 157

$(MPC)_w$ Values for Occupational Exposure to Sr^{90}, Sr^{89}, and Sr^{85} 157

Maximum Permissible Body Burdens and Maximum Permissible Concentrations Estimated by an Equivalence Relation Between External Dose and Internal Dose 163

$(MPC)_w$ for Rn^{222} 166

Maximum Permissible Concentration and Body Burden Values for Various Transuranic Radionuclides 169

Related Projects 175

17. STABLE-ELEMENT METABOLISM BY MAN 176

Influence of Age, Race, and Geographical Location on the Trace Element Concentration in Human Tissue 176

Tissue Analysis Laboratory Progress Report 178

PART V. HEALTH PHYSICS TECHNOLOGY

18. AEROSOL PHYSICS 185

Studies of Surface Contamination 185

Study of the Adsorption of Iodine Vapor onto Aerosols 187

Deposition of Dust in an Annular Impactor 189

Production of Submicron Aerosols 191

19. APPLIED INTERNAL DOSIMETRY 194

ORNL in Vivo Gamma-Ray Spectrometry Facility 194

Human Uptake and Excretion of I^{131}: Accidental Inhalation and Chronic and Single Ingestion of Iodine in Milk 194

Computer Program for in Vivo Counting Data 202

Developments in the ORNL in Vivo Gamma Ray Spectrometry Facility 204

Method for Removal of Alpha Contaminants in Phosphoric Acid 205

Iodine-131 in Milk and in Cattle Thyroids 206

PART VI. EDUCATION, TRAINING, AND CONSULTATION

20. EDUCATION, TRAINING, AND CONSULTATION 209

PAPERS, PUBLICATIONS, AND LECTURES

PAPERS 213

PUBLICATIONS 218

LECTURES 223

1147596

embled
iments
osime-
three
issell,
burgh;
ute of

Part IV. Internal Dosimetry

W. S. Snyder

147597

16. Estimation of Internal Dose

$(MPC)_w$ VALUES FOR OCCUPATIONAL EXPOSURE TO Sr^{90}, Sr^{89}, AND Sr^{85}

W. S. Snyder Mary Jane Cook
Mary R. Ford

Since the beginning of large-scale work with atomic energy, the metabolism of strontium has been the subject of intensive research efforts. The ICRP and NCRP Internal Dose Committees have recommended 2 μc as the maximum permissible body burden for Sr^{90}. In this study an attempt has been made to calculate occupational MPC values for Sr^{90}, Sr^{89}, and Sr^{85} which would limit the body burden of Sr^{90} to 2 μc over 50 yr of occupational exposure. No attempt has been made to assess the evidence concerning the carcinogenic potency of the strontium isotopes, but rather only the metabolic problem. Due to the lack of human data covering such an extended period, it is necessary to establish metabolic models. Several models have been considered, and the MPC values based upon each have been estimated. The first is a representation of the retention of a single intake to blood as a sum of three exponential functions; the second consists in using a power function to represent the retention; and the third involves the comparison of metabolism of calcium and strontium and centers about the observed ratio (OR), that is, $(Sr/Ca)_{bone}/(Sr/Ca)_{diet}$. Finally, data on stable strontium are considered and may be regarded in their own right as established directly, although only roughly, from the relation of intake and body burden.

The Exponential Model

In Table 16.1 the human studies which are the principal basis of the exponential model are summarized. According to the cited references, the subjects might be considered as "grossly normal" in all cases. No attempt was made here to study the many cases in which strontium metabolism has been studied in subjects who were aged or hospitalized for various ailments.

Figure 16.1 shows retention following a single intravenous injection of two individuals, "A" and "B," and an accidental puncture wound of the thumb in the case of the third individual, "C." In the case of "A" and "B" the radionuclide was Sr^{85}, which emits a 0.51-Mev gamma ray, so that retention was determined by whole-body counting. Fractional retention may also be estimated as 1 − excretion; however, this method is not considered as accurate as whole-body counting due to incomplete collection of excreta (i.e., sweat is known to include some of the material) and inaccuracies in analysis. It is found that the

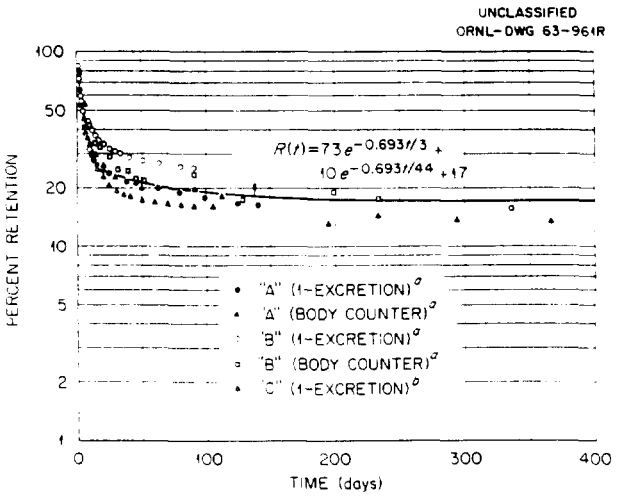

Fig. 16.1. Retention of Strontium Following Intravenous Administration. (Symbols *a* and *b* refer to footnotes of Table 16.1.)

1147598

Table 16.1. Description of Strontium Studies on Normal Human Subjects

Subject	Length of Study	Type of Analysis	Dose and Route of Entry	Comments
"A," "B"[a] (males; age, 47, 53; weight, ~80 kg)	140 days 1 yr	Excretion (fecal, urinary) Whole-body counting	Sr^{85} chloride; 0.5 μc; intravenously	"A" determined to be approximately in calcium balance
"C"[b] (male; age, 32; weight, ~84 kg)	115 days	Excretion (fecal, urinary)	(Sr^{90} + Y^{90} + Ca^{45}) chloride; puncture wound; 0.0074 μc (estimated)	Dietary calcium increased 2 to 3 times average after wound
"D," Japanese male[c,d] (age, 53; weight, ~68 kg)	163 days 212 days	Excretion (fecal, urinary) Whole-body counting	Sr^{85} chloride; ~5 μc; oral	Subject determined to be approximately in calcium balance
Sr-1, -2, -3[e] (males; age, adult; weight, ~74 kg)	160 days	Whole-body counting	Sr^{85}; 1.07 μc; oral	
"E" (REF)[e]	60 days	Whole-body counting	Sr^{85}; oral	
"F," "A"[f] (males; age, 40, 45; weight, 80, 85 kg)	20 to 25 days	Excretion (fecal, urinary)	Sr chloride, stable; intravenously; "F," 100 mg; "A," 20 mg	"A" determined to be approximately in calcium and strontium balance before study
"F," "B"[f] (males; age, 40, 50; weight, 85, 77 kg); "G" (female; age, 29; weight, 73 kg)	20 to 25 days	Excretion (fecal, urinary)	Sr chloride, stable; oral; males, 250 mg; "G," 100 mg	

[a]Margaret Bishop *et al.*, *Intern. J. Radiation Biol.* 2(2), 125 (1960).

[b]L. B. Farabee, *Health Phys. Div. Ann. Progr. Rept. July 31, 1961*, ORNL-3189, pp 224–26; L. B. Farabee and B. R. Fish, *Health Phys. Div. Ann. Progr. Rept. July 31, 1962*, ORNL-3347, pp 153–54; ORNL unpublished data.

[c]M. Fujita *et al.*, *Health Phys.* 9(4), 407 (1963).

[d]Susumu Suguri *et al.*, *Health Phys.* 9(5), 529 (1963).

[e]J. E. Furchner *et al.*, *Retention of Strontium-85 by Man*, LAMS-2780 (1962).

[f]G. E. Harrison, W. H. A. Raymond, and H. C. Tretheway, *Clin. Sci.* 14, 681 (1955).

formula

$$R(t) = 0.73e^{-0.693t/3} + 0.10e^{-0.693t/44} + 0.17 \quad (1)$$

fits the data rather well.

In the case of "C," Sr^{90} was accidentally injected, which meant that the intake was somewhat uncertain, and the retention was estimated only on the basis of excretion data. The shape of the retention curve for "C" is the most significant independent bit of information to be inferred from this exposure for the present purpose. It is seen that these three subjects have a reasonably consistent common pattern. The final constant term of Eq. (1) must be presumed to represent material which is being excreted from the body at a very

1147599

slow rate. On the basis of these data, it is not possible to determine whether this 17% consists of one, two, or three exponentials, but by analogy with radium, it must be supposed that some fraction of it will remain in bone after many years.

Before discussing the long-term retention, it is illuminating to consider the relation of Eq. (1) to the excretion data. These excretion data are shown in Fig. 16.2. The solid curve is the derivative of (1) except that the last term is taken as $0.17e^{-0.693t/4000}$, as discussed below. The agreement is remarkably good as excretion data go. It is likely that the low values measured are somewhat uncertain because of the very low level. Thus Eq. (1) seems adequate, so far as these individuals are concerned, for interpretation of the early metabolism of strontium ($t < 200$ days).

If the 17% retained at about 1 yr is the sum of several components with different elimination rates, the replacement of these exponentials by a single exponential will lead to the same body burden as the use of several, provided the elimination rate is chosen to achieve this. Assuming that all this material is eliminated slowly (half-life long compared to a year), then the error will not be a gross one if all such components are grouped together. For example, if one had $0.07e^{-0.693t/10} + 0.10e^{-0.693t/20}$ instead of $0.17e^{-0.693t/20}$ (time in years), then in 50 yr the error in the body burden would be 20%. Thus the short-term studies only fix the size of the long-term-retention component, but with this size fixed, one may use an average rate of elimination for it and hope to estimate the body burden with reasonable accuracy provided one long-term retention value can be estimated to represent an average rate of elimination over this period.

Data on stable strontium provide such a check value provided the model can be modified suitably for oral intakes. Figure 16.3 shows excretion data on "B" and "F," who took stable strontium both intravenously and orally. The excretion values do differ by a fairly consistent factor over the entire period of observation. To avoid exogenous material and the uncertainty of the lowest values, the two sets of values have been averaged over the period from 4 to 20 days. The ratio of the average values was found to be 0.36.

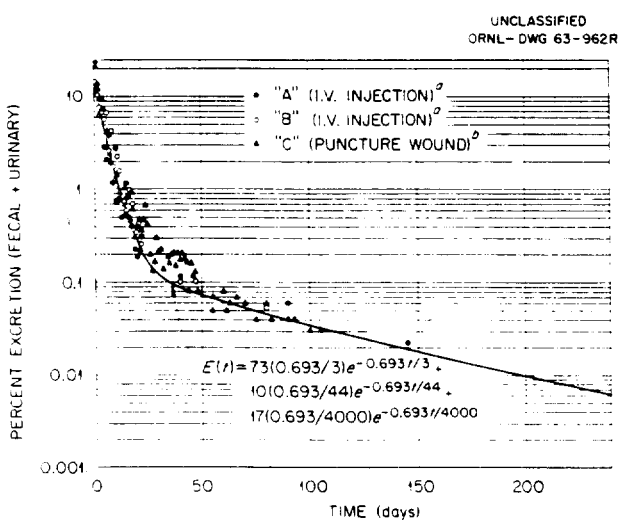

Fig. 16.2. Excretion of Strontium Following Intravenous Administration. (Symbols *a* and *b* refer to footnotes of Table 16.1.)

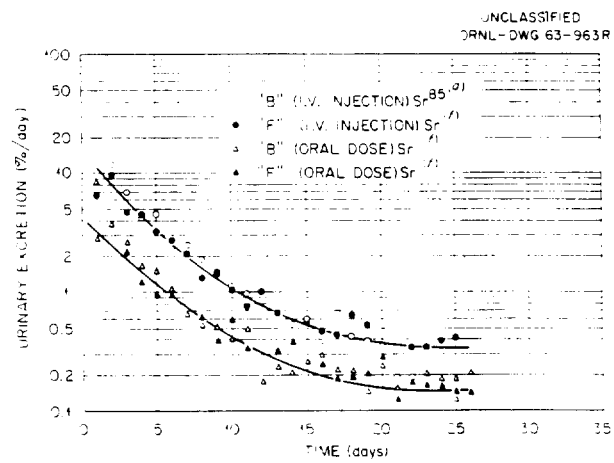

Fig. 16.3. Urinary Excretion of Strontium Following Oral or Intravenous Administration. (Symbols *a* and *f* refer to footnotes of Table 16.1.)

Figure 16.4 shows data on five male adults who took Sr^{85} orally. Equation (1) has been modified by a suitably chosen factor f_1 in each case, and it has been found that the data do tend to follow the formula when so adjusted. Thus the use of a constant factor, that is, a constant percentage shift of all portions of the curve, seems a reasonable assumption. It will be noted that the values of f_1 that must be used range from 0.17 to 0.5.

1147600

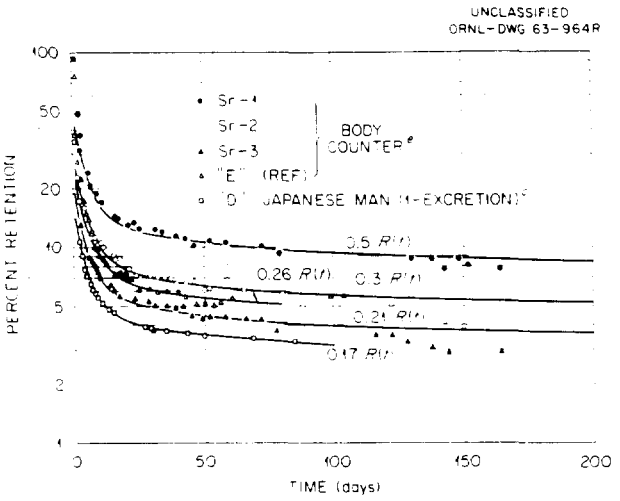

Fig. 16.4. Retention of Strontium after Oral Administration. (See Table 16.1, footnotes c and e.)

Table 16.2 shows data on the Sr/Ca ratio in diet and bone. These data undoubtedly leave much to be desired. In many cases the number of individual samples is small, and in no case is it known whether or not an individual that contributed a bone sample really consumed something like the diet which was sampled. Despite these grave shortcomings, it may be that these data are the best human data now available on the long-term accumulation of a body burden of strontium. It must be remembered that the standard man can only represent some kind of average or typical individual, and thus it is somewhat more excusable to use "average" values of diet and bone samples to obtain his elimination rate.

The English data predict that the adult body burden should average 209 daily intakes, and the total of United States data would predict 182 daily

Table 16.2. $(MPC)_w$ for Sr^{90} Estimated from Diet-Bone Data on Stable Strontium

Bone				Food			
Source of Sample	Sample Size	Responsible for Analysis	μg of Sr per g of Ca	Source of Sample	Responsible for Analysis	Intake (mg/day)	$(MPC)_w$ (μc/ml)
							$\times 10^{-6}$
San Francisco	24	ORNL	378	San Francisco	HASL	1.90	4.6
San Francisco	5	HASL	300	San Francisco	HASL	1.90	5.8
Chicago	4	ORNL	286	Chicago	HASL	1.82	5.8
Chicago	6	HASL	290	Chicago	HASL	1.82	5.8
New York	6	HASL	250	New York	HASL	1.53	5.6
New York	127	Lamont	410	New York	HASL	1.53	3.4
United States	171	ORNL	320	Av { New York, San Francisco, Chicago }	HASL	1.75	4.5
England	31	Harwell	355	England	British Agricultural Research Council	1.6	4.3
Montreal		Chalk River	280	Canada	Chalk River	1.3	4.2
San Juan	5	HASL	503	San Juan	HASL	1.23	2.2

1147601

intakes. Since the data on American diets are less extensive (as represented here), it may be better at present to use the British data. If this is done directly, the daily intake to produce a body burden of 2 μc of Sr^{90} is at least 2/209 μc/day = 9.5×10^{-3} μc/day. The corresponding $(MPC)_w = 9.5 \times 10^{-3}/2200 = 4.3 \times 10^{-6}$ $\mu c/cm^3$, 168 hr/week. These values are conservative on several counts: (1) no allowance is made for radioactive decay, and (2) the young adult has already accumulated a considerable body burden of stable strontium. Nevertheless, the value must be regarded as highly uncertain. The data on U.S. diets and bone would give $(MPC)_w = 5.1 \times 10^{-6}$ $\mu c/cm^3$, 168 hr/week.

Returning to the exponential model and assuming a state of equilibrium, the body burden for unit daily intake with $f_1 = 0.3$ would be

$$0.3 \left[\frac{0.73 \times 3}{0.693} + \frac{0.10 \times 44}{0.693} + \frac{0.17 \times T_b}{0.693} \right] ;$$

setting the above result equal to 210, one obtains $T_b = 2800$ days. Most British experimenters report $f_1 \approx 0.20$ (ref 1), and if this is used, one obtains $T_b = 4300$ days. Thus a value of T_b of the order of 3000 to 4000 days seems indicated by the dietary-bone data. The U.S. data would give a smaller value.

One other bit of data, again somewhat tenuous, may be used to check on the long-term elimination rate. Rowland has estimated an average turnover rate of 3 to 5% a year for bone.[2] Although the bone samples may not be representative of total bone and of "standard" man, it seems worthwhile to see if it is grossly out of line with the above model. The average turnover rate of the long-term compartment is $0.693/T_b \times 365 \times 100\%$ per year. With $T_b = 3000$ this amounts to 8%, and for $T_b = 4000$, to about 6%. The value of $T_b = 4000$ is preferred here, partly because of this slightly closer agreement with Rowland's estimate and partly because the MPC it determines is more conservative. Even if the U.S. "standard" man has $f_1 = 0.3$, one obtains $(MPC)_w = 4.3 \times 10^{-6}$ $\mu c/cm^3$, 168 hr/week.

[1] J. F. Loutit, *Irradiation of Mice and Men*, The University of Chicago Press, 1962.

[2] R. E. Rowland, p 339 in *Radioisotopes in the Biosphere* (ed. by R. S. Caldecott and L. A. Snyder), University of Minnesota, Minneapolis, 1960.

Power-Function Model

Power-function models for retention have been given by ICRP Committee II,[3] by Marinelli,[4] and by Bishop *et al.*[5] The retention function given by Bishop *et al.*[5] more closely resembles the animal models as summarized by Rowland.[6] The $(MPC)_w$ values for Sr^{90} corresponding to these retention functions are given below.

If the retention function following intravenous administration is $R(t) = at^{-b}$, then the body burden following 50 yr of intake of I μc/day is given by

$$q(t) = If_1 \int_0^t d\tau\, a(t-\tau)^{-b}\, e^{-\lambda_r(t-\tau)}$$

$$= If_1 \int_0^t dx\, ax^{-b} e^{-\lambda_r x} ,$$

where $t = 50 \times 365$. Using the function as recommended by Marinelli, $R(t) = 0.95t^{-0.25}$, and taking $q = 2$ μc and $f_1 = 0.3$, one obtains for Sr^{90} $I = 5.7 \times 10^{-3}$ and $(MPC)_w = 2.6 \times 10^{-6}$ $\mu c/cm^3$, 168 hr/week. The formula $R(t) = 0.65t^{-0.35}$ given in *ICRP, Report of Committee II* yields $I = 1.8 \times 10^{-2}$ μc/day and $(MPC)_w = 8.3 \times 10^{-6}$ $\mu c/cm^3$, 168 hr/week. The formula $R(t) = 0.51t^{-0.23}$ given by Bishop *et al.*[5] yields $I = 8.5 \times 10^{-3}$ μc/day and $(MPC)_w = 3.9 \times 10^{-6}$ $\mu c/cm^3$, 168 hr/week.

Comparison with Calcium

Many investigators have reported that

$$OR = (Sr/Ca)_{bone}/(Sr/Ca)_{diet} \cong 0.25 .$$

It is known that the value of the observed ratio can be perturbed by grossly altering the diet. However, for a normal diet the value of 0.25 has been considered as rather well established. Nevertheless, the bone-diet data reported from HASL (Table 16.2) yield lower values, but again the sampling is not very extensive. If OR = 0.25 is used to estimate

[3] *Report of Committee II on Permissible Dose for Internal Radiation*, ICRP Publication 2, Pergamon, London, 1959.

[4] L. D. Marinelli, *Estimates of Bone Pathology to Be Expected from Sr^{90}*, ANL-5716 (1957).

[5] Margaret Bishop *et al.*, *Intern. J. Radiation Biol.* 2(2), 125 (1960).

[6] R. E. Rowland, *Retention and Plasma Clearance of the Alkaline Earth Elements*, ANL-6104, pp 34–37 (1959).

1147602

Table 16.3. Reported Observed Ratio Values

Observed Ratio (OR)	Method	Reference
0.2–0.25	Hospital patients; double tracer Ca^{45} and Sr^{85}	J. L. Kulp and A. R. Schulert, *Sr^{90} in Man and His Environment. Part I*, NYO-9934, pp 152–53 (May 1962).
0.25	Comparison of diet and bone levels	J. L. Kulp and A. R. Schulert, *Science* **136**, 619 (1962).
0.25	Stable strontium and calcium, Wales and north and west England	F. J. Bryant, A. C. Chamberlain, and G. S. Spicer, *Brit. Med. J.* **1958**, 1371.
0.23	Stable strontium and calcium, England	J. D. Burton and E. R. Mercer, *Nature* **193**, 846 (1962).
0.16	Stable strontium and calcium in adults, New York	J. Rivera, *Fallout Program Quarterly Summary Report April 1, 1963–July 1, 1963*, HASL-138, pp 235–38.
0.16	Stable strontium and calcium in adults, Chicago	
0.16	Stable strontium and calcium in adults, San Francisco	
0.2	Stable strontium and calcium in adults, San Francisco	ORNL unpublished data to W. S. Snyder from S. R. Koirtyohann and C. Feldman, 1962; J. Rivera, *Fallout Program Quarterly Summary Report April 1, 1963–July 1, 1963*, HASL-138, pp 235–38.
0.16	Stable strontium and calcium in adults, Chicago	
0.18	Stable strontium and calcium in adults, average for U.S.	
0.16	Japanese	Y. Hiyama, quoted by J. D. Burton and E. R. Mercer, *Nature* **193**, 846 (1962).
0.18	Stable strontium and calcium; human rib samples from U.S.	G. V. Alexander and R. E. Nussbaum, *J. Biol. Chem.* **234**, 418 (1959).
0.35	Double tracer Sr^{85} and Ca^{45}; hospital patients	Herta Spencer, D. Laszlo, and M. Brothers, *J. Clin. Invest.* **36**, 680 (1957).
0.53	Double tracer Sr^{85} and Ca^{45}	C. L. Comar *et al.*, *Proc. Soc. Exptl. Biol. Med.* **95**, 386 (1957).
0.35	Double tracer Sr^{85} and Ca^{45}; two patients on nonmilk diets	C. L. Comar, R. S. Russell, and R. H. Wasserman, *Science* **126**, 485 (1957).
0.31	Stable strontium and calcium in infants (0–1 yr); New York	J. Rivera, *Fallout Program Quarterly Summary Report April 1, 1963–July 1, 1963*, HASL-138, pp 235–38.
0.48	Stable strontium and calcium in infants (0–1 yr); Chicago	
0.31	Stable strontium and calcium in infants (0–1 yr) San Francisco	
Body/diet, average = 0.92; std deviation = ±0.27; range, 0.54–1.48	Fourteen infants; at beginning of observation period, ages ranged from 25 to 46 days	S. A. Lough, J. Rivera, and C. L. Comar, *Proc. Soc. Exptl. Biol. Med.* **112**, 631 (1963).

1147603

uptake and retention of strontium, the intake to give a uniform labeling of the skeleton at the level of 2 μc burden is (μc of Sr^{90} per g of Ca)$_{diet}$ · OR × (g of Ca in standard man) = q (μc of Sr^{90}), that is,

$$(I/1) \cdot 0.25 \cdot 10^3 = 2$$

or

$$I = 8 \times 10^{-3}\ \mu c/\text{day}\ .$$

This gives an $(MPC)_w = 3.6 \cdot 10^{-6}\ \mu c/cm^3$, 168 hr/week. The value is conservative insofar as it neglects radioactive decay of Sr^{90}.

The observed ratio (OR) model is very attractive on several counts. First, it purports to control the local concentration of strontium in the bone, since the model assumes that the new bone formed will be at the level of the plasma at the time of formation. For constant exposure level this would ensure a nearly uniform concentration. Moreover this model is the one of the four discussed here that seems most immediately applicable to the child or the infant. With the other models it must be assumed that the parameters might change with age. There is the possibility that the OR may be greater, particularly during the first year following birth. Some human data as well as some animal studies have suggested such a change.[7,8] If this discrimination exists, it is supposed to be partially offset by placental discrimination and, in any case, is easily taken into account for application to infants. Table 16.3 lists various OR values that have been reported, from which it is seen that the value of 0.25 is rather conservative. However, some of the lower values rest on relatively few samples.

Sr^{89} and Sr^{85}

Merely by changing the radioactive half-life, the $(MPC)_w$ values for Sr^{89} and Sr^{85} are readily obtained either by the power-function model or from the exponential model. It is not so easy to adapt the OR model or the direct data on diet and bone since no elimination rate is implied by the model. The $(MPC)_w$ values obtained from the exponential and power-function models are listed in Table 16.4.

Table 16.4. $(MPC)_w$ Values for Sr^{90}, Sr^{89}, and Sr^{85} as Computed by Various Models[a]

Model	Radionuclide		
	Sr^{90}	Sr^{89}	Sr^{85}
	$\times 10^{-6}$	$\cdot 10^{-4}$	$\times 10^{-3}$
$R(t) = 0.65t^{-0.35}$	8.3	4.1	6.2
$R(t) = 0.95t^{-0.25}$	2.6	2.1	3.0
$R(t) = 0.51t^{-0.23}$	3.9	3.6	5.3
$R(t) = 0.73e^{-0.693t/3} + 0.10e^{-0.693t/44} + 0.17e^{-0.693t/4000}$	4.3	3.3	4.7
OR	3.6		
Diet-bone data (British)	4.3		
Diet-bone data (U.S.)	4.5		
NCRP values (Handbook 69)	1	1	1

[a] $\mu c/cm^3$, 168 hr/week; critical organ, bone.

MAXIMUM PERMISSIBLE BODY BURDENS AND MAXIMUM PERMISSIBLE CONCENTRATIONS ESTIMATED BY AN EQUIVALENCE RELATION BETWEEN EXTERNAL DOSE AND INTERNAL DOSE

S. R. Bernard

The purpose in this work is to suggest a possible method for estimating the maximum permissible body burden, q, and maximum permissible concentration, MPC, for Sr^{90} from a different model than the critical-organ concept employed by ICRP and NCRP. Use is made of the toxicity data on mice published by Finkel[9] and of Henshaw's[10] life-shortening data from chronic whole-body external exposure of mice to x rays. With these data an equivalence between external exposure and internal exposure can be derived; then from the

[7] A. C. Andersen, *The Effects of Continual Sr^{90} Ingestion During the Growth Period of the Beagles and Its Relation to Ra^{226} Toxicity*, UCD-106 (June 1962).

[8] R. J. Della Rosa and R. Pool, *Radiation Res.* 19(1), 179 (1963).

[9] M. P. Finkel, *Proc. Second Intern. Conf. Peaceful Uses At. Energy* **22**, 65 (1958).

[10] P. S. Henshaw, *J. Natl. Cancer Inst.* **4**, 521 (1944).

1147604

life-shortening data on American radiologists,[11] this equivalence relation can be extrapolated to man, and some estimates can be made of an equivalent q and MPC for man.

The equivalence relation between external external exposure and internal exposure is based on Henshaw's data in Fig. 16.5, which presents a plot of R, the roentgens per day external exposure of mice, vs the median life span S in days. The equation fitted to the data is

$$R = 40 \left| \frac{1 - (S/320)}{1 - e^{-0.7S/37}} \right| , \qquad (1)$$

[11] Discussed in *Report of the United Nations Scientific Committee on the Effects of Atomic Radiation*, suppl No. 16 (A/5216), p 144, 1962.

in r/day, and it is a fairly adequate representation over the entire region. In this equation the life span S_0 of control animals is ~320 days. With $x = S/S_0$ and values of $x \to 1$, the equation simplifies to

$$R \sim 40(1 - x) , \qquad (2)$$

in r/day.

An expression similar to (1) can be obtained from a fit of Finkel's Sr^{90} data. Figure 16.6 shows a plot of the single-injection dose q_0/m, in μc/g, into mice vs the median life span S, in days. The equation fitted to Finkel's data is

$$q_0/m = \left| \frac{1 - (S/600)}{1 - e^{-0.7S/180}} \right| , \qquad (3)$$

in μc/g. Here S_0 is 600 days. For values of

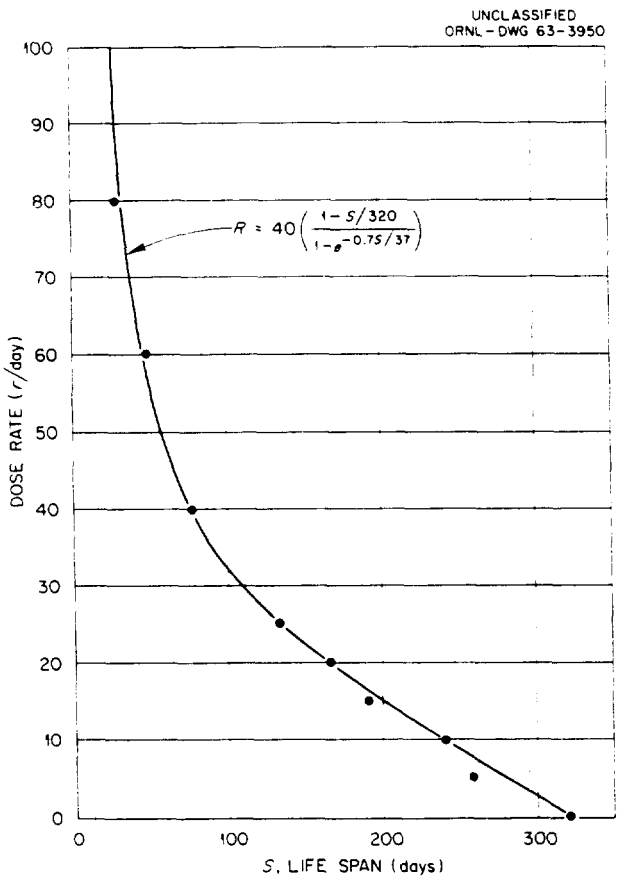

Fig. 16.5. Henshaw's Data; Mice, Chronic Irradiation (X Rays).

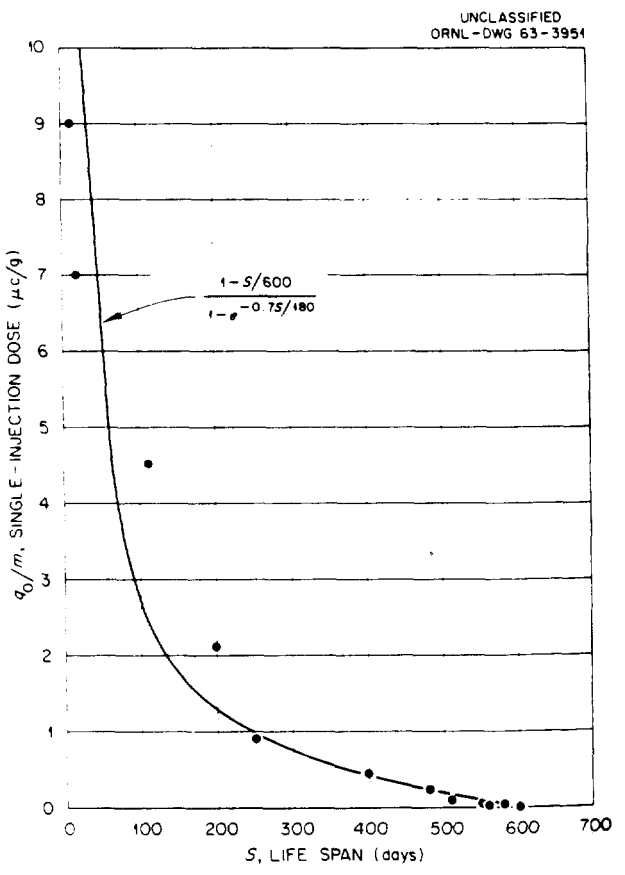

Fig. 16.6. Finkel's Strontium Data; Mice, Injection Dose (μc/g) vs Survival Time (days).

1147605

$S/S_0 = x \to 1$, the expression

$$q_0/m \sim (1 - x) , \qquad (4)$$

in μc/day, is a fair representation.

From (2) and (4), x can be eliminated, and we obtain the equivalence

$$q_0/m = R/40 . \qquad (5)$$

From this equation, we may say that a single-injection dose of 1 μc of Sr^{90} per g of body weight produces the same percentage of life shortening in mice as does chronic, external, whole-body exposure of mice to 40 r/day. We can use this expression to estimate q_0 and MPC for man *if we can assume that the same equivalence relation between external dose and internal dose in man would hold.* However, some extrapolation from mouse to man must be made. Use is made of the data on American radiologists to extrapolate formula (1) for man.

Braestrup[12] has estimated the external dose to American radiologists of ~100 rads/yr (0.4 rad/day). Their average life span was 60.5 yr. Other physicians had a life span of ~65.7 yr. Thus, the fractional life span

$$x = \frac{60.5}{65.7} = 0.921 .$$

From (2) we would find that $R = 3.16$ r/day when $x = 0.921$. We can equate the absorbed dose rate, rads/day, to the exposure dose rate since the mice were exposed to 200-kvp x rays. Thus, mice require eight times the dose rate that man does to give a fractional life span of 0.921. A similar check on the extrapolation of (4) is desirable, but corresponding data on man are not available. The permissible external dose rate for man is 0.1 rad/week (0.02 rad/day, occupational exposure), which is equivalent to 0.16 rad/day exposure of mice. From (5) we estimate q_0/m equivalent to 0.16 rad/day and obtain

$$q_0/m = \frac{0.16}{40} = 0.004 ,$$

in μc/g. This would suggest that man could take 0.004 μc/g × 70,000 g = 280 μc as a single injection, and the injury in terms of life shortening would be equivalent to that resulting from exposure to 0.1 rad/week, *providing this equivalence relation holds for man* and the above extrapolation from mouse to man is valid. The bone burden would be 0.3 × 280 μc ≅ 84 μc. (Here the value of 0.3, the fraction going from blood to bone, was taken from *ICRP, Report of Committee II.*) The body burden would be 84/0.99 ≅ 84 μc since f_2, the fraction in the bone to that in the body, which is also taken from the handbook, is given as 0.99. This value of 84 μc is not comparable with the 2-μc value recommended by ICRP and NCRP for body burden that results from chronic intake.

To estimate an $(MPC)_w$, actually, we should have continuous ingestion data on mice to construct a plot of the $\mu c/cm^3$ vs the median life span and employ a similar equivalence relation. For a crude estimate we can calculate the daily incremental amount put into man over a period of 50 yr such that the total intake would be 280 μc. In 50 yr there are 200 quarters, and the quarterly intake would be 280/200 μc per quarter = 1.4 μc per quarter. This is the input into the blood. Since only 0.3 is assumed to be absorbed from the gut into blood, then man could ingest 1.4/0.3 = 4.6 μc per quarter. This is to be compared with the permissible quarterly intake of 0.2 μc recommended by ICRP and NCRP. It is a factor of 23 times higher.

Note in this equivalence-relation method no adjustment for radiological decay is made. The value of q_0 indicates an amount which can be put into the body but only as a single quantity or parceled out over a period of 50 yr of exposure. Thus, insofar as the q_0 value is concerned, no direct comparison with the usual body burden should be made. As for the $(MPI)_w$ value (quarterly permissible intake in water), it is permissible to compare this value with the ICRP or NCRP recommendations. It would appear that the ICRP or NCRP recommendations are conservative. However, this estimation method should not be used without checking with data on more species of animals which were administered lower injection levels or which experienced continuous feeding and inhalations of the radionuclides. In addition to the need for data to permit interspecies extrapolation, other biological effects should be considered also. When such data become available, a more firm basis for conclusions about q and MPC may evolve.

[12] Cited by P. R. J. Burch, *Nature* **185**, 135–42 (1960).

1147606

$(MPC)_w$ FOR Rn^{222}

S. R. Bernard

In a previous progress report[13] an $(MPC)_w$ for Rn^{222} was estimated to be $\sim 2 \cdot 10^{-4}$ $\mu c/cm^3$ based on yellow bone marrow which was considered as a blood-forming organ. This is now believed to be a factor of 2.5 too low because the decay chain of Rn^{222} contains chiefly alpha emitters whose ranges are short enough so that the energy will be dissipated in the yellow marrow and not in the nearby red marrow. Thus, a revision upward by a factor of 2.5 is suggested in order to prevent compounding of safety factors.

$(MPC)_w$ values for various organs and tissues based on Nussbaum's[14] experimentally determined f_2 values have been calculated and appear in Table 16.5. For these calculations the method of estimation previously described[13] was employed. As can be noted, fat and yellow marrow are the critical organs, and the $(MPC)_w$ is 5×10^{-4} $\mu c/cm^3$ (168 hr/week) for occupational exposure.

The dose to the stomach has also been considered, for which Nussbaum does not have measurements. The ICRP model was employed for

[13] S. R. Bernard, *Health Phys. Div. Ann. Progr. Rept. July 31, 1961*, ORNL-3189, p 192.

[14] E. Nussbaum, *Radon Solubility in Body Tissues and in Fatty Acids*, UR-503 (1957).

Table 16.5. $(MPC)_w$ for Occupational Workers Exposed 168 hr/week

Organ	m (g)[a]	f_2	m/f_2	R (rem/week)	$(MPC)_w$ ($\mu c/cm^3$)
			$\times 10^5$		$\times 10^{-3}$
Muscle	30,000	0.07	4.3	0.1	5.2
Skin	6,100	0.01	6.1	0.3	22
Fat	10,000	0.71	0.14	0.3	0.5
Skeleton	7,000	0.016	4.4	0.3	16
Red marrow	1,500	0.0095	1.6	0.1	1.9
Yellow marrow	1,500	0.11	0.14	0.3	0.5
Blood	5,400	0.035	1.5	0.3	5.4
GI tract	2,000	0.092	2.2	0.3	7.9
Liver	1,700	0.008	2.1	0.3	7.6
Brain	1,500	0.007	2.1	0.3	7.6
Lungs	1,000	0.004	2.5	0.3	9
Lymphoid tissue	700	0.003	2.3	0.3	8.3
Kidneys	300	0.0012	2.5	0.3	9
Heart	300	0.0011	2.7	0.3	9.7
Spleen	150	0.0006	2.5	0.1	3
Urinary bladder	150	0.0003	5	0.3	18
Testes	70	0.0001	4	0.1	4.8
Balance	884	0.004	2.2	0.3	7.9
Total body	70,000	1	0.7	0.1	0.84

[a] From *ICRP Handbook*, p 151.

1147607

estimating the dose to the stomach, which was determined not to be a critical organ. However, the ICRP model does not take into account the possibility of diffusion of inert gases into the

burden by f_2, the fraction of that in the total body present in the kidneys, in which case an estimate of f_2 is available in the handbook. Or another way, from the equation $gf_2 = 2.8 \times 10^{-3}\ RM/\epsilon$,

and since I_i will be the same for all daughters (assuming equilibrium with Rn^{222} at the time of ingestion) and because λ_i^r is relatively large, the first term of (6) is negligible and (6) simplifies to

$$q_i \sim q_{i-1} \,. \tag{7}$$

Now from Eq. (5), p 194, ORNL-3189, we obtain q_0, and inserting q_0 into Eq. (7) gives

$$q_1 = \frac{(\mathrm{MPC})_w}{8.3 \times 10^{-3}}\ \mu c = q_2 = q_3 = q_4 \,. \tag{8}$$

Since $(\mathrm{MPC})_w = 5 \times 10^{-4}\ \mu c/cm^3$,

$$q_i = 0.06\ \mu c\,, \qquad i = 0, 1, 2, 3, 4 \,. \tag{9}$$

Thus we have at equilibrium 0.06 μc of Rn^{222} and each of its short-lived daughters present in the body. Now we must calculate the permissible q_i for each of the short-lived daughters, for which we need values of f_2, m, and ϵ. Since the kidney is the critical organ for each of these daughters, m = 300 g, and the value of f_2 can be obtained from Table 12 of the *ICRP Handbook*. The value of ϵ is computed from a table of isotopes by Strominger, Hollander, and Seaborg.[19]

Table 16.6 presents the calculated values of q. The first column shows the isotope; the second column shows the value of ϵ estimated by the procedures set forth in Sec VI of the *ICRP Handbook*; the third, the f_2 value; and the fourth, the value of q calculated from Eq. (1). As can be seen in the fourth column, the permissible body burden for Po^{218} is 0.06 μc present in the body from decay of Rn^{222}. Also, the 0.05-μc burden permissible for Po^{214} is slightly lower than the 0.06 μc present. Thus, these calculations indicate that the $(\mathrm{MPC})_w$ of $5 \times 10^{-4}\ \mu c/cm^3$ is too high since the body burdens of the short-lived polonium daughters are too high, and, subsequently, the kidneys would receive an exposure of ~0.6 rem/week from the short-lived polonium daughters produced by decay of Rn^{222}.

In the kidney dose estimation, from Table 16.6 it is noted that the $(\mathrm{MPC})_w$ for Rn^{222} would have

Table 16.6. Values of q for the Short-Lived Daughters of Rn^{222} Based on Kidneys as the Critical Organ

Isotope	ϵ (Mev)	f_2[a]	q (μc)
Po^{218}	62	0.067	0.06
Pb^{214}	<0.4[b]	0.13	5[c]
Bi^{214}	<1.6[b]	0.3	0.5[c]
Po^{214}	80	0.067	0.05

[a]Estimated from Eq. (41) in the *ICRP Handbook* and data in Table 12 and assuming $T^x = T^t$.

[b]These energies are slight upper-bound estimates of ϵ because they were based on the body as the organ of reference; since they have large gamma components in their decay scheme, the energy absorption will be less in kidneys because of their smaller dimensions.

[c]These are lower-bound estimates because the value of ϵ employed in their calculation is somewhat too high.

to be lowered by about a factor of 2 to prevent the overirradiation of kidney tissue from uptake of short-lived polonium daughters. However, we find that the $(\mathrm{MPC})_w$ might have a hidden safety factor of about 2.2 contained in it, and, due to this and the extreme conservatism in the assumption, it is not necessary to reduce the $(\mathrm{MPC})_w$. The factor of 2.2 comes from considering a daily intake of 2200 cm^3/day for water – a customary procedure – but in fact the standard man only consumes 1000 cm^3 of fluids per day (Table 9 of the *ICRP Handbook*). The other 1200 cm^3 comes from intake of foods. Arguing that in the processing of foods Rn^{222} would have greater chances to escape by diffusion during heating, decay by sitting on shelves, and loss by other kinds of processing, then it would seem that we should employ 1000 cm^3 rather than 2200 cm^3 as the daily intake. Thus we apparently have a safety factor of at least 2 in the $(\mathrm{MPC})_w$ for Rn^{222} (minus its daughters). Hence, it is not necessary to reduce by a factor of 2 the $(\mathrm{MPC})_w$ based on radiation exposure of kidneys by the polonium daughters. Also, in making the above calculations we were extremely conservative in assuming that a short-lived polonium atom formed anywhere in the body will reach the kidney to undergo disintegration. It seems more probable that the 3-min half-life of Po^{218} would perhaps be long enough to favor its transferring from, say,

[19]D. J. Strominger, J. M. Hollander, and G. T. Seaborg, *Table of Isotopes*, UCRL 1928 (2nd Rev); *Radiological Health Handbook*, pp 195–454, U. S. Dept. Health, Education and Welfare, Public Health Service, September 1960.

1147609

fat in a limb to kidney rather than the 1.6×10^{-4} sec Po^{214}, which would probably disintegrate at or near the site of its production.

The question of dose to the lungs from exhalation of ingested Rn^{222} must be considered too. In order to estimate this dose we need to know the fraction f of the daughters in the lung air which exists as free ions. This is evidently not known as no experimental data for this case were found. However, we can make a crude estimate of dose by considering the following argument. Since the daily intake of Rn^{222} by ingestion is $5 \times 10^{-4} (\mu c/cm^3) \times 2200 (cm^3/day) = 1.1\ \mu c/day$, assuming 2200-$cm^3$/day intake, and since ~99% of this is eliminated by the body (we assume via exhalation), the μc/day exhaled by a worker ingesting the $(MPC)_w$ is $0.99 \times 1.1 = 1.0\ \mu c/day$.

The standard man exhales $2 \times 10^7\ cm^3/day$, and thus the concentration of Rn^{222} exhaled is

$$\frac{1.0}{2 \times 10^7} = 5 \times 10^{-8}\ \mu c/cm^3 .$$

A worker who inhales the $(MPC)_a$ for Rn^{222} (equal to $10^{-8}\ \mu c/cm^3$) would be expected in the steady state to exhale about the same concentration, that is, $10^{-8}\ \mu c/cm^3$. This level is a factor of 5 lower than the level exhaled by the worker who chronically ingests the $(MPC)_w$.

The calculation of lung dose implies that the lungs are overexposed to radiation. However, the $(MPC)_a$ is for the case of inhalation of Rn^{222} *and its daughters* and depends upon the level at which the radium A daughter exists in the form of free ions, since these unattached atoms deliver all but a small fraction of the dose to the bronchi of lungs. For inhalation of Rn^{222} and daughters, the *ICRP Handbook* (p 23) uses the formula

$$(MPC)_a = \frac{3 \times 10^{-6}}{1 + 1000f}\ \mu c/cm^3 \text{ (40-hr week)} ,$$

where f is the fraction of the equilibrium amount of radium A ions which are unattached to nuclei. In the case of Rn^{222} that originates in the deep parts of the lung, we do not have an experimental value for f. Provided that f is not larger than 0.02, the dose rate delivered to lungs from ingested Rn^{222} at the level of $5 \times 10^{-4}\ \mu c/cm^3$ will not be in excess of the permissible dose rate. It seems unlikely that f could be as high as 0.02, since there is probably little time for the decay of Rn^{222} atoms to form radium A atoms (i.e., a turnover time for lung air is probably much less than the half-life of the radium A daughter, so that radium A could not equilibrate with Rn^{222}), and because of the presence of a high concentration of water vapor relative to ordinary air in exhaled air, serving as nuclei for attachment of radium A atoms. However, this is mere speculation, and an experimental measurement of f for this case would be required to estimate adequately the dose to lungs from exhalation of ingested Rn^{222}.

In view of the following considerations, that is, there is a possibility that the dose to kidneys might be as high as ~0.6 rem/week from deposition of short-lived daughters and that the lungs could possibly be overexposed due to exhalation of Rn^{222}, it does not seem to be advisable to remove the safety factor of 2 and increase the $(MPC)_w$. When more adequate data are made available, then if it is indicated that neither the kidneys nor the lungs will be overexposed, an increase in the $(MPC)_w$ can be justified.

MAXIMUM PERMISSIBLE CONCENTRATION AND BODY BURDEN VALUES FOR VARIOUS TRANSURANIC RADIONUCLIDES

Mary R. Ford W. S. Snyder

Maximum permissible concentrations in air, $(MPC)_a$, and in water, $(MPC)_w$, and body burden limits, q, have been computed for occupational exposure to 20 radionuclides of importance in the Transuranium Program. The specific radionuclides were U^{240}, Pu^{243}, Pu^{244}, Am^{242m}, Am^{242}, Am^{244}, Cm^{247}, Cm^{248}, Cm^{249}, Bk^{250}, Cf^{251}, Cf^{253}, Cf^{254}, Es^{253}, Es^{254m}, Es^{254}, Es^{255}, Fm^{254}, Fm^{255}, and Fm^{256}. The basic biological and physical assumptions which are the basis of the calculations were adopted after discussion with Committee II of ICRP and Subcommittee 2 of NCRP and conform to their recommendations. Values were tabulated in each case for (1) insoluble material, using both the lungs and the GI tract as organs of reference, and for (2) soluble material, using total body, bone, GI tract, and other organs wherever indicated as organs of reference. The computations were made according

1147610

to the formulas and assumptions of the NCRP[20] and ICRP[21] internal-dose reports. In cases where the radionuclide decays to a stable state through a chain of radioactive daughters, the computations become quite involved, and originally these determinations were programmed for the Oracle. However, since the Oracle was being disassembled when the transuranic computations were needed, the problem was reprogrammed for the IBM 7090 computer.

Biological data used in the computations were taken from Table 12 of the *ICRP, Report of Committee II*,[21] where these data were given, that is, for U, Pu, Am, Bk, and Cf. The literature was searched for biological data for the other transuranics, Es and Fm, and none were found, no doubt because of the small quantity of material available for study. However, since the chemical properties of any one of the transcurium elements are known to be very similar to those of the rest,[22] the assumption was made that the biological properties were similar; and, thus, the biological parameters for these elements were taken to be identical to the values given in the *ICRP, Report of Committee II* for Bk and Cf. The biological parameters for each radionuclide and each organ of reference considered were listed in a table entitled "Biological and Related Physical Constants."

Physical data for determining radioactive half-lives, type and mode of decay, and energy quantities and intensities were taken principally from refs 23 and 24. Energies absorbed by the various organs of reference were computed from these data and listed in a table entitled "Effective Energies." In conformity with recommendations of ICRP[21] these energies were weighted by RBE; by n, the relative damage factor for radionuclides deposited in bone; and by F, the ratio of disintegrations of daughter atoms to the disintegrations of the parent. A more detailed table entitled "Effective Energies for Chains" was also included which gave the breakdown of F values (as computed by the IBM 7090) and average energies multiplied by RBE and n for parent-daughter chains.

One problem arose with the new group of radionuclides that was not encountered in the previous group. This was the matter of radionuclides in which the prominent mode of decay is spontaneous fission. A survey of the pertinent literature revealed that the quantity and distribution of spontaneous fission energy for most of the radionuclides involved are not precisely known as yet. However, it has been shown both theoretically and experimentally[25] that the energy release in spontaneous fission is similar to the energy release in the neutron-induced fission of U^{235}. The approximate distribution[26] of neutron-induced fission energy is:

Energy Group	Mev
1. Kinetic energy of fission fragments	168 ± 5
2. Instantaneous gamma-ray energy	5 ± 1
3. Kinetic energy of fission neutrons	5 ± 0.5
4. Beta particles from fission products	7 ± 1
5. Gamma rays from fission products	6 ± 1
6. Neutrinos	~10
Total fission energy	201 ± 6

The energy in groups (1), (2), and (3) is released at the time of fission (considering for this purpose the time of the delayed neutrons as negligible), while that in groups (4) and (5) is set free gradually as the fission products decay. Since neutrinos do not interact appreciably with matter, the energy from that source can be neglected.

The calculations that involved spontaneous fission in the present list made use of data contained in Table 16.7. Since not all the spontaneous fission energy distributions for the different

[20] *Maximum Permissible Body Burdens and Maximum Permissible Concentrations of Radionuclides in Air and in Water for Occupational Exposure*, NBS Handbook 69, Superintendent of Documents, Washington, 1959.

[21] *Report of Committee II on Permissible Dose for Internal Radiation*, ICRP Publication 2, Pergamon, London, 1959.

[22] G. H. Higgins, *The Radiochemistry of the Transuranic Elements*, AEC Nuclear Science Series NAS-NS 3031 (1960).

[23] E. K. Hyde, *The Radioactive Decay of the Isotopes of the Transuranium Elements*, UCRL-9148 (January 1961); UCRL-9036 (January 1960).

[24] Landolt-Bornstein, *New Series, Energy Levels of Nuclei: A = 5 to A = 257*, Springer-Verlag, Berlin, 1961.

[25] A. B. Smith, P. R. Fields, and A. M. Friedman, *Phys. Rev.* 104(3), 699 (1956).

[26] Samuel Glasstone, *Principles of Nuclear Reactor Engineering*, p 22, Van Nostrand, New York, 1955.

1147611

Table 16.7. Distribution of Spontaneous Fission Energy

	Radionuclide					
	U^{235} (neutron induced)	Pu	Cm	Cf	Es	Fm
Kinetic energy of fragments, Mev[a]	167		(180)[b]	185	(180)	176
ν, neutrons per fission[a]	2.42		(2.8)	3.86	(3.95)	4.05
Energy per neutron,[a] average-Mev	2.0		(2)	2.15	(2.18)	2.2
Total gamma-ray energy per fission[a]						
Prompt, average-Mev	7.5 (first few μsec)		(9)	9	(9)	(8.5)
Delayed, average-Mev	(+10 to 20% for gammas up to a millisecond)		(+10 to 20%)	(+10 to 20%)	(+10 to 20%)	(+10 to 20%)
Energy, prompt gammas per fission,[a] average-Mev	0.8		(0.8)	0.8–0.9	(~0.9)	(~0.9)
Total average beta energy from fission products per fission,[c] Mev	7.6	(7.5)	(7.4)	(7.0)	(7.0)	(7.0)
Energy per beta,[c] average-Mev	1.2	(1.17)	(1.12)	(1.05)	(1.05)	(1.05)
Total gamma energy from fission products per fission,[c] Mev	6.0	(5.8)	(5.6)	(5.2)	(5.2)	(5.2)
Energy per fission product gamma,[c] average-Mev	1.6 at 10^2 sec 0.5 at 10^5 sec Average ~1.3	(1.26)	(1.19)	(1.15)	(1.15)	(1.15)

[a]From literature survey by H. W. Schmitt, private communication.
[b]Values in parentheses were estimated from measured values of neighboring elements.
[c]From literature survey by G. D. O'Kelley, private communication.

isotopes of an element are known at present but are considered to be quite similar,[27] the values given in the table for an element have been used for all isotopes of that element. Also, in cases where values are not available from the literature for an element, for example, plutonium, values were extrapolated from those used for neighboring elements in Table 16.7. Such values in the table are enclosed in parentheses.

In keeping with the assumptions of the NCRP[20] and ICRP[21] internal-dose reports, n was taken as 1 and 5 for the gamma and beta radiations, respectively, arising from spontaneous fission. Since the kinetic energy of the fragments and the neutron components was considered to be as damaging as alpha rays, n was taken equal to 5 for these energies. An RBE of 20 was used

[27]H. W. Schmitt and G. D. O'Kelley, private communication.

1147612

for the kinetic energy of fission fragments. This value was recommended by ICRP Committee II at its meeting in New York, September 1961. Using Fig. 14 of the *United States National Bureau of Standards Handbook 63* as a guide, RBE for spontaneous fission neutrons was taken equal to 8; and, as in the internal-dose reports, 1 was used for the beta and gamma components. In computing effective energies for the GI tract, only 1% of the kinetic energy release of the fission fragments was included since it was assumed that this energy, like the energy from alpha particles, would fail to penetrate the mucosa to an appreciable extent.

Both the NCRP and ICRP committees have reviewed the material on the transuranics in regard to basic philosophy, format, and parameters used; and after certain revisions resulting from an interchange of ideas, the ICRP committee has adopted the values listed here. They also will appear in the forthcoming ICRP Publication 6, *Recommendations of the International Commission on Radiological Protection, as Amended 1959 and Revised 1962.* Subcommittee 2 of NCRP has these values under consideration. Only the values of MPC and q are given in Table 16.8.

Table 16.8. Maximum Permissible Body Burdens and Maximum Permissible Concentrations of Radionuclides in Air and Water for Occupational Exposure

Radionuclide and Type of Decay	Solubility	Organ of Reference[a]	Maximum Permissible Burden in Total Body, q (μc)	Maximum Permissible Concentrations (MPC)			
				40-hr Week		168-hr Week	
				Water (μc/cm^3)	Air (μc/cm^3)	Water (μc/cm^3)	Air (μc/cm^3)
$_{92}U^{240} + Np^{240}$	sol	GI(LLI)		10^{-3}	2×10^{-7}	3×10^{-4}	8×10^{-8}
$\alpha, \beta^-, \gamma, e^-$		Kidney	4	0.4	2×10^{-6}	0.1	5×10^{-7}
		Total body	20	2	10^{-5}	0.8	4×10^{-6}
		Bone	2	3	10^{-5}	1	4×10^{-6}
	insol	GI(LLI)		10^{-3}	2×10^{-7}	3×10^{-4}	6×10^{-8}
		Lung			10^{-6}		5×10^{-7}
$_{94}Pu^{243}$	sol	GI(ULI)		0.01	2×10^{-6}	3×10^{-3}	6×10^{-7}
$\alpha, \beta^-, \gamma, e^-$		Bone	7	10^3	10^{-5}	400	5×10^{-6}
		Kidney	30	5×10^3	7×10^{-5}	2×10^3	2×10^{-5}
		Liver	40	6×10^3	7×10^{-5}	2×10^3	3×10^{-5}
		Total body	50	8×10^3	10^{-4}	3×10^3	4×10^{-5}
	insol	GI(ULI)		2×10^{-6}	2×10^{-6}	3×10^{-3}	8×10^{-7}
		Lung		0.01	2×10^{-5}		6×10^{-6}
$_{94}Pu^{244}$	sol	Bone	0.04	10^{-4}	2×10^{-12}	4×10^{-5}	6×10^{-13}
$\alpha, \beta^-, \gamma, e^-$ (99.7%);		GI(LLI)		3×10^{-4}	7×10^{-8}	10^{-4}	2×10^{-8}
spontaneous		Kidney	0.4	6×10^{-4}	8×10^{-12}	2×10^{-4}	3×10^{-12}
fission (0.3%)		Total body	0.3	9×10^{-4}	10^{-11}	3×10^{-4}	4×10^{-12}
	insol	Lung			3×10^{-11}		10^{-11}
		GI(LLI)		3×10^{-4}	6×10^{-8}	10^{-4}	2×10^{-8}
$_{95}Am^{242m}$	sol	Bone	0.07	10^{-4}	6×10^{-12}	4×10^{-5}	2×10^{-12}
$\alpha, \beta^-, \gamma, \epsilon, e^-$		Kidney	0.1	10^{-4}	6×10^{-12}	5×10^{-5}	2×10^{-12}
		Liver	0.3	2×10^{-4}	9×10^{-11}	7×10^{-5}	3×10^{-12}
		Total body	0.3	3×10^{-4}	2×10^{-11}	10^{-4}	5×10^{-12}
		GI(LLI)		3×10^{-3}	6×10^{-7}	9×10^{-4}	2×10^{-7}
	insol	Lung			3×10^{-10}		9×10^{-11}
		GI(LLI)		3×10^{-3}	5×10^{-7}	9×10^{-4}	2×10^{-7}

1147613

Table 16.8 (continued)

Radionuclide and Type of Decay	Solubility	Organ of Reference[a]	Maximum Permissible Burden in Total Body, q (μc)	Maximum Permissible Concentrations (MPC) 40-hr Week Water ($\mu c/cm^3$)	40-hr Week Air ($\mu c/cm^3$)	168-hr Week Water ($\mu c/cm^3$)	168-hr Week Air ($\mu c/cm^3$)
$_{95}Am^{242}$ $\alpha, \beta^-, \gamma, \varepsilon, e^-$	sol	GI(LLI)		4×10^{-3}	8×10^{-7}	10^{-3}	3×10^{-7}
		Liver	0.06	0.9	4×10^{-8}	0.3	10^{-8}
		Kidney	0.1	2	8×10^{-8}	0.6	3×10^{-8}
		Bone	0.1	2	8×10^{-8}	0.6	3×10^{-8}
		Total body	0.3	4	2×10^{-7}	1	6×10^{-8}
	insol	Lung			5×10^{-8}		2×10^{-8}
		GI(LLI)		4×10^{-3}	7×10^{-7}	10^{-3}	2×10^{-7}
$_{95}Am^{244}$ $\alpha, \beta^-, \gamma, e^-$	sol	GI(SI)		0.1	3×10^{-5}	0.05	10^{-5}
		Bone	0.2	90	4×10^{-6}	30	10^{-6}
		Kidney	0.2	100	4×10^{-6}	30	10^{-6}
		Liver	0.2	100	5×10^{-6}	40	2×10^{-6}
		Total body	0.4	200	10^{-5}	80	3×10^{-6}
	insol	Lung			2×10^{-5}		8×10^{-6}
		GI(SI)		0.1	2×10^{-5}	0.05	8×10^{-6}
$_{96}Cm^{247}$ $\alpha, \beta^-, \gamma, e^-$	sol	Bone	0.04	10^{-4}	5×10^{-12}	4×10^{-5}	2×10^{-12}
		Liver	0.5	2×10^{-4}	9×10^{-12}	7×10^{-5}	3×10^{-12}
		Kidney	0.2	2×10^{-4}	9×10^{-12}	7×10^{-5}	3×10^{-12}
		Total body	0.4	3×10^{-4}	10^{-11}	10^{-4}	5×10^{-12}
		GI(LLI)		6×10^{-4}	10^{-7}	2×10^{-4}	5×10^{-8}
	insol	Lung			10^{-10}		4×10^{-11}
		GI(LLI)		6×10^{-4}	10^{-7}	2×10^{-4}	4×10^{-8}
$_{96}Cm^{248}$ α(89%); spontaneous fission (11%)	sol	Bone	5×10^{-3}	10^{-5}	6×10^{-13}	4×10^{-6}	2×10^{-13}
		Liver	0.06	2×10^{-5}	10^{-12}	8×10^{-6}	4×10^{-13}
		Kidney	0.03	3×10^{-5}	10^{-12}	9×10^{-6}	4×10^{-13}
		Total body	0.04	4×10^{-5}	2×10^{-12}	10^{-5}	6×10^{-13}
		GI(LLI)		4×10^{-5}	8×10^{-9}	10^{-5}	3×10^{-9}
	insol	Lung			10^{-11}		4×10^{-12}
		GI(LLI)		4×10^{-5}	7×10^{-9}	10^{-5}	2×10^{-9}
$_{96}Cm^{249}$ $\alpha, \beta^-, \gamma, e^-$	sol	GI(S)		0.06	10^{-5}	0.02	5×10^{-6}
		Bone	1	300	10^{-5}	100	4×10^{-6}
		Total body	4	800	3×10^{-5}	300	10^{-5}
	insol	GI(S)		0.06	10^{-5}	0.02	4×10^{-6}
		Lung			5×10^{-5}		2×10^{-5}
$_{97}Bk^{250}$ $\alpha, \beta^-, \gamma, e^-$	sol	GI(ULI)		6×10^{-3}	10^{-6}	2×10^{-3}	5×10^{-7}
		Bone	0.05	10	10^{-7}	4	5×10^{-8}
		Total body	0.3	80	10^{-6}	30	4×10^{-7}
	insol	GI(ULI)		6×10^{-3}	10^{-6}	2×10^{-3}	4×10^{-7}
		Lung			2×10^{-6}		8×10^{-7}

1147614

Table 16.8 (continued)

Radionuclide and Type of Decay	Solubility	Organ of Reference[a]	Maximum Permissible Burden in Total Body, q (μc)	Maximum Permissible Concentrations (MPC) 40-hr Week Water ($\mu c/cm^3$)	40-hr Week Air ($\mu c/cm^3$)	168-hr Week Water ($\mu c/cm^3$)	168-hr Week Air ($\mu c/cm^3$)
$_{98}Cf^{251}$ α, γ	sol	Bone	0.04	10^{-4}	2×10^{-12}	4×10^{-5}	6×10^{-13}
		GI(LLI)		8×10^{-4}	2×10^{-7}	3×10^{-4}	6×10^{-8}
		Total body	0.3	9×10^{-4}	10^{-11}	3×10^{-4}	4×10^{-12}
	insol	Lung			10^{-10}		3×10^{-11}
		GI(LLI)		8×10^{-4}	10^{-7}	3×10^{-4}	5×10^{-8}
$_{98}Cf^{253}$ $\alpha, \beta^-, \gamma, e^-$	sol	GI(LLI)		4×10^{-3}	9×10^{-7}	10^{-3}	3×10^{-7}
		Bone	0.04	0.06	8×10^{-10}	0.02	3×10^{-10}
		Total body	0.3	0.5	6×10^{-9}	0.2	2×10^{-9}
	insol	Lung			8×10^{-10}		3×10^{-10}
		GI(LLI)		4×10^{-3}	7×10^{-7}	10^{-3}	3×10^{-7}
$_{98}Cf^{254}$ Spontaneous fission	sol	GI(LLI)		4×10^{-6}	8×10^{-10}	10^{-6}	3×10^{-10}
		Bone	7×10^{-4}	4×10^{-4}	5×10^{-12}	10^{-4}	2×10^{-12}
		Total body	5×10^{-3}	3×10^{-3}	4×10^{-11}	10^{-3}	10^{-11}
	insol	Lung			5×10^{-12}		2×10^{-12}
		GI(LLI)		4×10^{-6}	6×10^{-10}	10^{-6}	2×10^{-10}
$_{99}Es^{253}$ $\alpha, \beta^-, \gamma, e^-$	sol	GI(LLI)		7×10^{-4}	10^{-7}	2×10^{-4}	5×10^{-8}
		Bone	0.04	0.06	8×10^{-10}	0.02	3×10^{-10}
		Total body	0.3	0.4	5×10^{-9}	0.1	2×10^{-9}
	insol	Lung			6×10^{-10}		2×10^{-10}
		GI(LLI)		7×10^{-4}	10^{-7}	2×10^{-4}	4×10^{-8}
$_{99}Es^{254m}$ $\alpha, \beta^-, \gamma, e^-$	sol	GI(LLI)		5×10^{-4}	10^{-7}	2×10^{-4}	4×10^{-8}
		Bone	0.02	0.4	5×10^{-9}	0.1	2×10^{-9}
		Total body	0.1	3	4×10^{-8}	1	10^{-8}
	insol	Lung			6×10^{-9}		2×10^{-9}
		GI(LLI)		5×10^{-4}	10^{-7}	2×10^{-4}	3×10^{-8}
$_{99}Es^{254}$ $\alpha, \beta^-, \gamma, e^-$	sol	GI(LLI)		4×10^{-4}	9×10^{-8}	10^{-4}	3×10^{-8}
		Bone	0.02	10^{-3}	2×10^{-11}	5×10^{-4}	6×10^{-12}
		Total body	0.2	10^{-2}	10^{-10}	3×10^{-3}	5×10^{-11}
	insol	Lung			10^{-10}		4×10^{-11}
		GI(LLI)		4×10^{-4}	7×10^{-8}	10^{-4}	3×10^{-8}
$_{99}Es^{255}$ α, β^-, γ	sol	GI(LLI)		8×10^{-4}	2×10^{-7}	3×10^{-4}	6×10^{-8}
		Bone	0.04	0.04	5×10^{-10}	0.01	2×10^{-10}
		Total body	0.3	0.3	4×10^{-9}	0.09	10^{-9}
	insol	Lung			4×10^{-10}		10^{-10}
		GI(LLI)		8×10^{-4}	10^{-7}	3×10^{-4}	5×10^{-8}

1147615

Table 16.8 (continued)

Radionuclide and Type of Decay	Solubility	Organ of Reference[a]	Maximum Permissible Burden in Total Body, q (μc)	Maximum Permissible Concentrations (MPC) 40-hr Week Water ($\mu c/cm^3$)	40-hr Week Air ($\mu c/cm^3$)	168-hr Week Water ($\mu c/cm^3$)	168-hr Week Air ($\mu c/cm^3$)
$_{100}Fm^{254}$	sol	**GI(ULI)**		4×10^{-3}	8×10^{-7}	10^{-3}	3×10^{-7}
α, γ, e^- (99.9448%);		Bone	0.02	5	6×10^{-8}	2	2×10^{-8}
spontaneous		Total body	0.1	30	4×10^{-7}	10	2×10^{-7}
fission	insol	**Lung**			7×10^{-8}		2×10^{-8}
(5.52×10^{-2}%)		**GI(ULI)**		4×10^{-3}	6×10^{-7}	10^{-3}	2×10^{-7}
$_{100}Fm^{255}$	sol	**GI(LLI)**		10^{-3}	2×10^{-7}	3×10^{-4}	7×10^{-8}
α, γ		**Bone**	0.04	1	2×10^{-8}	0.4	6×10^{-9}
		Total body	0.3	9	10^{-7}	3	4×10^{-8}
	insol	**Lung**			10^{-8}		4×10^{-9}
		GI(LLI)		10^{-3}	2×10^{-7}	3×10^{-4}	6×10^{-8}
$_{100}Fm^{256}$	sol	**GI(ULI)**		3×10^{-5}	6×10^{-9}	9×10^{-6}	2×10^{-9}
Spontaneous		Bone	8×10^{-4}	0.2	3×10^{-9}	0.07	10^{-9}
fission		Total body	5×10^{-3}	1	2×10^{-8}	0.5	7×10^{-9}
	insol	**Lung**			2×10^{-9}		6×10^{-10}
		GI(ULI)		3×10^{-5}	5×10^{-9}	9×10^{-6}	2×10^{-9}

[a]The abbreviations GI, S, SI, ULI, and LLI refer to gastrointestinal tract, stomach, small intestine, upper large intestine, and lower large intestine respectively; critical organ is in bold-face type.

RELATED ACTIVITIES

Members of the Internal Dose Estimation Section have participated in the iodine studies reported by the Health Physics Technology Section, in the Clinch River Survey Program Evaluation Study reported by the Radioactive Waste Disposal Section, and in the program of High-Energy-Proton Dosimetry carried out under NASA and reported in the Radiation Physics and Dosimetry Section.

During the year several members of the Section have participated in two meetings of the National Committee on Radiation Protection Subcommittee 2. The Section also has assisted in the preparation of material for the forthcoming Publication 6 of the International Commission on Radiological Protection.

Members of the Section have participated in conferences held at Argonne Cancer Research Hospital and at Hanford Atomic Operations on the Biology of Radioiodine and at similar conferences on program reviews at Wayne State University and at The Lovelace Foundation.

One member of the Section serves as Editor-in-Chief of the journal *Health Physics* and another serves as Editor.

In cooperation with the Education and Training Section, one member presented six lectures and another presented four lectures in the AEC Fellowship Course of Applied Radiation Physics, Vanderbilt University, Nashville, Tennessee.

Two members each presented one lecture at the University of Tennessee for Physics 599E, Seminars in Health Physics.

1147616

17. Stable-Element Metabolism by Man

INFLUENCE OF AGE, RACE, AND GEOGRAPHICAL LOCATION ON THE TRACE ELEMENT CONCENTRATION IN HUMAN TISSUE

Isabel H. Tipton Mary Jane Cook
Jane Shafer

Data from spectrographic analysis of trace elements in the tissues of children from the United States, India, and Africa, of caucasoid and negroid adults from the United States and Africa, and of caucasoid adults from India have been treated statistically by nonparametric methods which have been described elsewhere.[1] In tests of variation, adult males of the same age group (20–59 yr) but from different geographical locations or of different races were compared. All children (0–19 yr), male and female, from one location were compared with all adults, male and female, from the same location. Females from one location were compared with males of the same age (20–59 yr) from the same location. Table 17.1 shows the number of individuals in each group and the number of samples of aorta, kidney, liver, and lung for which data were available.

On the whole the concentrations of trace elements in children were not different from those in adults, but certain elements in certain tissues showed significant variations.

Calcium in aorta was significantly lower (probability $p \leqq 0.01$) in the American children than in the American adults, but the two samples of aorta available from Indian children were not different from those from Indian adults with respect to this element. (No samples of aorta from African children were analyzed.) The median value for the calcium in aorta for American children was lower than that for the African and Indian adults. This value for the American adults, however, was significantly higher ($p \leqq 0.01$) than for the African and Indian adults.

Concentrations of cadmium in kidney were significantly lower ($p \leqq 0.01$) in the children of each group. The median concentration of this

[1] I. H. Tipton *et al.*, *Health Phys.* 9(2), 89 (1963).

Table 17.1. Number of Individuals and Organs from Each Group

		Adults (20–59 yr)					Children (0–19 yr)				
		Total	Aorta	Kidney	Liver	Lung	Total	Aorta	Kidney	Liver	Lung
United States	All subjects[a]	118	80	115	118	113	23	8	21	22	22
	All females	30	21	27	29	27					
	Male, caucasoid	52	40	52	52	51					
	Male, negroid	21	12	21	21	21					
Africa	All subjects	49	15	44	41	40	5	0	5	4	5
	All females	15	2	12	11	12					
	Male, caucasoid	4	4	4	4	4					
	Male, negroid	30	9	28	26	24					
India	All subjects	29	10	23	26	26	9	2	9	9	9
	Female, caucasoid	5	1	4	4	4					
	Male, caucasoid	24	9	19	22	22					

[a] Fifteen subjects, race unknown.

1147617

element in the kidneys of American children, however, was slightly higher than that for the African adults. Cadmium in liver was lower in children also, but this difference was not so highly significant as that for kidney.

Lead showed interesting variations (see Figs. 17.1–17.3). In the group of children from the United States, lead was consistently significantly lower than it was in adults, while in the groups of children from India and from Africa, this element showed no significant difference in any tissues. In the American group, tissues of males showed higher lead than the same tissues of females, and negroid males showed higher lead in lung and liver than caucasoid males. American males in general showed higher lead than African or Indian males. These differences in the levels of lead reflect the difference in exposure to lead in the atmosphere. Butt and his colleagues have observed that the concentration of lead in serum is higher the longer the period of daily travel in an automobile.[2]

There appeared to be no significant differences due to race *per se*. Except for the higher lead in lung and kidney (which is probably a reflection of occupational exposure), the American negroid group was not significantly different ($p \leq 0.01$) from the American caucasoid group in any respect. The African negroids differed from African caucasoids at this level of significance only in higher calcium in kidney and molybdenum in liver. On the other hand, the American negroids were significantly different ($p \leq 0.01$) from African negroids for many elements, and the American caucasoids were significantly different ($p \leq 0.01$) from the African caucasoids for approximately the same elements. The Africans were higher in aluminum in aorta, kidney, and liver and much lower in cadmium and lead in kidney, liver, and lung. The Indian caucasoids did not differ from the African negroids in as many respects nor as significantly as they did from the American caucasoids. The

[2]Private communication.

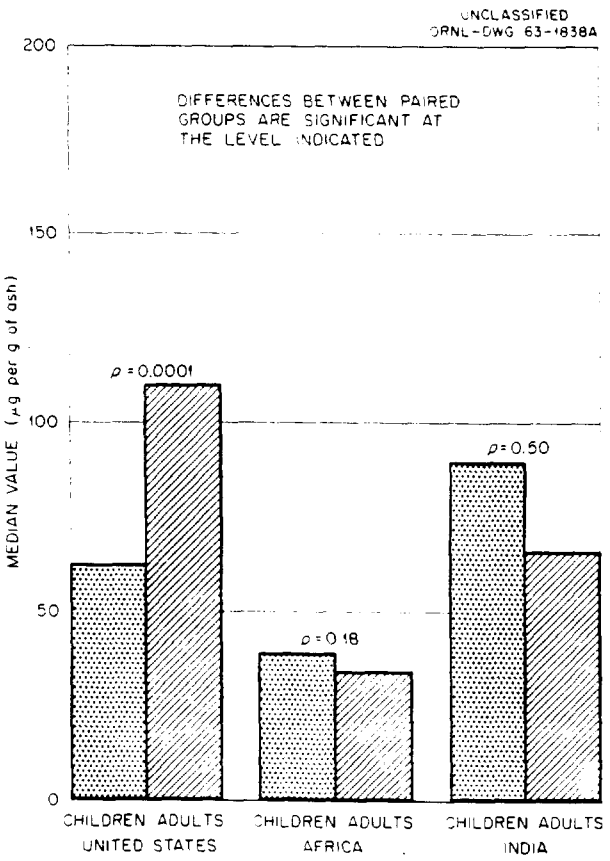

Fig. 17.1. Lead in Kidney, Age Differences.

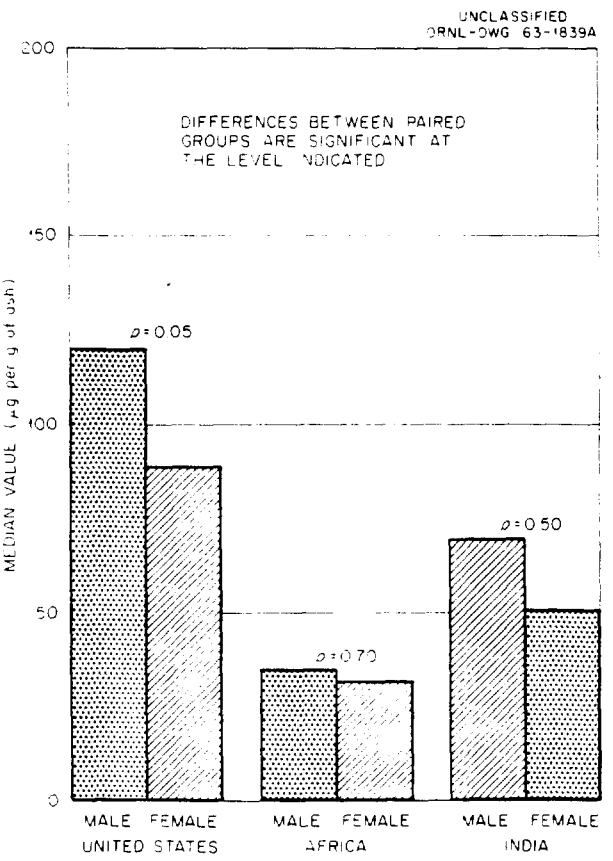

Fig. 17.2. Lead in Kidney, Sex Differences.

1147618

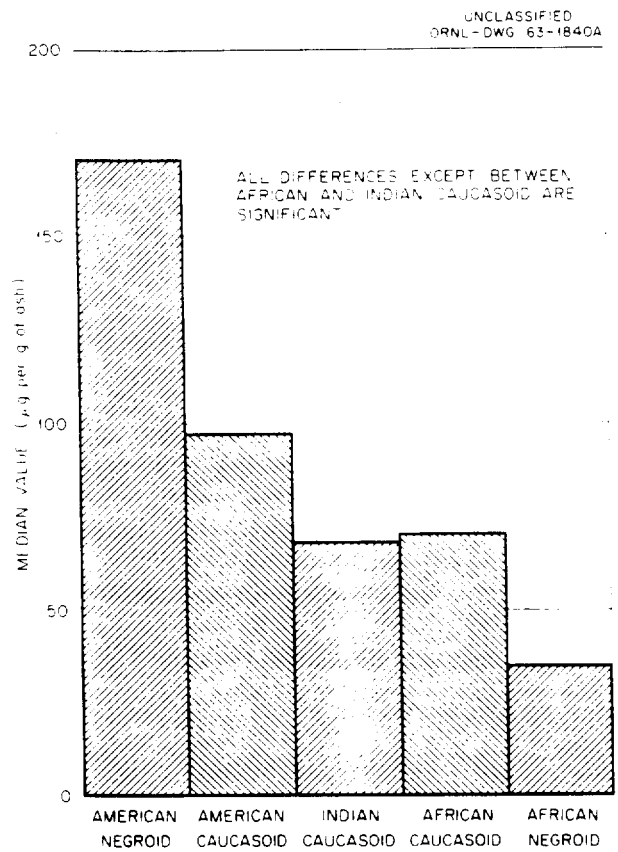

Fig. 17.3. Lead in Kidney, Geographic and Race Differences.

differences between the American subjects and the African and Indian subjects are not surprising in view of the differences in diet and nutritional status and the differences in exposure to contaminants.

Except for higher lead ($p \leq 0.05$) in kidney, liver, and lung of males, there were no sex differences in the American group. The African females had significantly higher ($p \leq 0.01$) cadmium in kidney than African males. The Indian males and females showed no significant differences.

TISSUE ANALYSIS LABORATORY PROGRESS REPORT

S. R. Koirtyohann C. Feldman

During the past year about 415 bone samples were analyzed for 20 elements by three different procedures. The trace elements were determined by the method previously described.[3] Sodium and calcium were determined in solutions of these samples using a flame as the light source on the Quantometer. Potassium was determined in these same solutions by use of a conventional flame spectrophotometer. Phosphorus values were obtained from the San Francisco bone samples by a colorimetric method.

The data obtained from the San Francisco bone samples are given in Table 17.2. These data show much less variability than the soft tissues in the values for Mg, Sr, Zn, Ca, P, and Na in the ash. This is especially true in the case of Ca and P, where the extreme values are less than 10% different from the average.

A few bone samples were analyzed repeatedly over a period of several months to test the long-term reproducibility of the method used for the trace element determinations. Standard deviations were calculated in the cases where the data were sufficiently complete. They are summarized below:

Standard Deviation (%)	No. of Values
<5	2
5–10	7
10–20	8
>20	1

The precision of the flame methods used for the Na, Ca, and K determinations is much better than this (≈ 2%).

The accuracy of the Quantometer values was checked for several elements by using independent methods. The results for iron and strontium are given in Table 17.3, and other comparisons are discussed below.

In addition to the analysis of bone samples, about 400 samples of soft tissues from Atlanta and New York and 36 samples of whole blood from the New Jersey Department of Health[4] were analyzed for 23 trace elements. These blood samples were from people who had been employed in the radium-dial-painting factories. A cursory comparison indicated that these values were within the range usually regarded as normal.

[3] W. S. Snyder *et al.*, *Health Phys. Ann. Progr. Rept. July 31, 1962*, ORNL-3347, p 109.

[4] These samples were supplied through the courtesy of L. A. Barrer, Director, Radium Research Project.

1147619

Table 17.2. Analyses of San Francisco Bone Samples

Concentrations are expressed as μg per gram of ash except for Na, Ca, K, and P, which are as percent in the ash. Numbers in parentheses are estimates from photographic exposures.

ORNL Sample No.	% Dry	% Ash	Co	Fe	Cu	Ni	Cr	Pb	Al	Mn	Mo	Sn	Mg	Sr	Ba	Zn	Cd	Au	%Na	%Ca	%K	%P
300 B	76	31		320	(10)			33	28	(2)			5000	99		190			1.10	36.8	0.50	18.4
302 B	58	14		1200	10	(2)		96	46	(3)		(5)	5800	120		240			1.62	34.0	0.96	16.2
303 B	67	24		350	(5)	(2)		140	(15)	(2)			5100	160		220			1.66	36.0	0.79	16.2
304 B	72	26		500	(5)			34	(20)	(2)			4200	91		180			1.14	35.4	0.54	16.4
305 B	66	29		150	(20)			46	(20)	(2)		(5)	4800	120		160			1.23	35.3	0.56	16.4
306 B	63	25		540	(5)			70	22	(2)			5600	120		180			1.46	37.4	0.66	16.4
307 B	65	34		100				(10)	(20)	(2)			5300	120		140			1.06	35.5	0.39	17.5
308 B	58	23		660	(2)			77	32	(2)			5600	120		200			1.18	36.8	0.75	17.2
309 B	74	32		540	13			30	(20)	(2)			4900	120		200			1.18	36.2	0.39	17.2
310 B	80	35		400	(2)			64	27	(2)		(20)	5000	220		200			1.18	36.2	0.36	17.2
312 B	76	46		180				(10)	(15)	(2)			4000	160		130			1.09	37.9	0.23	17.5
313 B	54	15		860	(5)	(2)		71	23	(5)			5200	180		230			1.70	34.5	0.86	17.0
314 B	81	33		160	(2)			30	24	(3)		(10)	4400	140		190			1.06	36.4	0.34	17.2
315 B	61.7	25.1		660	(2)			76	(5)	(2)			4800			270			1.53	32.9	0.56	15.5
316 B	66	32		320	(2)			46	(15)	(2)		(5)	5000	160		160			1.04	36.2	0.44	17.0
317 B	63	26		520	(5)			46	(10)	(2)		(5)	4400	130		160			1.50	34.4	0.56	16.2
319 B	64	23		480	(2)			32	(10)	(2)		(5)	5000	120		200			1.14	35.9	0.54	17.8
320 B	66	28		950	(2)	(5)		30	(30)	(2)			5200	110		160			1.12	35.8	0.58	17.0
321 B	69	28		910	(2)			67	(15)	(2)			4900	130		180			1.25	37.3	0.40	17.2
322 B	69	27		540	(2)			28	(15)	(2)			4600	89		150			1.22	36.6	0.30	17.5
323 B	73	24		600				70	(10)	(2)			4500	220		140			1.22	36.2	0.66	17.2
324 B	64	25		280	(2)			62	(10)	(2)		(20)	4400	160		170			1.29	37.2	0.44	17.2
325 B	64	27		410	(2)			40	(10)	(2)		(10)	3900	120		180			1.29	34.7	0.40	16.2
326 B	67	24		480	(2)			63	(10)	(3)			4400	110		180			1.28	37.0	0.48	17.0
327 B	76	28		410				39	(5)	(2)		(10)	4900	170		200			1.25	34.9	0.39	17.0
Av	58	27		494	4.3			51	19	2.3			4800	130		180			1.27	35.9	0.52	17.0
Detection limits			(2)	(20)	(2)	(2)	(2)	(5)	(5)	(2)	(2)	(5)		(1)	(20)	(50)	(5)	(2)				

1147620

Table 17.3. Colorimetric and Flame-Spectrophotometric Values for Iron and Strontium in Bone

Sample No.	Fe		Sr	
	Quantometer	Colorimetric	Quantometer	Flame
302 B	1200	970	120	120
303 B	350	315	160	140
304 B	500	470	91	92
305 B	150	175	120	125
306 B	540	540	120	115

Radium was not determined. An average of 2.2 ppm of Sr in whole blood ash was reported. This is believed to be one of the first values published for Sr in blood and should be checked against blood from persons who have not been employed in the radium dial factories. Gofman[5] reported a 0.00-ppm value in serum.

Atomic absorption spectroscopy is a very valuable tool for checking the accuracy of the Quantometer values for several elements. In this method light of proper wavelength is passed through a flame into which the sample solution is aspirated. Atoms of the test element, which are liberated in the flame, absorb the light and reduce the intensity by an amount proportional to their concentration. This method is capable of very good sensitivity. Concentrations as low as single parts per billion (10^{-9} g/ml) of some elements can be detected in the sample solution. Detection limits based on concentrations in the ash are generally not as good as in the arc because a rather dilute solution of the ash (0.1–1.0%) must be used. Interferences and interelement effects are generally much less serious than with other spectrochemical methods. Precision of 1–2% of the amount present can be obtained under favorable conditions. The method yields results on only one element at a time and is not applicable to elements that form refractory oxides in the flame (Al, Ti, Si).

[5] J. W. Gofman, p 1 in *Advances in Biological and Medical Physics*, vol VIII (ed. by C. A. Tobias and J. H. Lawrence), Academic Press, New York, 1962.

The atomic absorption method has been used to check the Quantometer values for Zn, Pb, Cd, and Mn in soft tissues and for Zn and Mg in bone. The results from the soft tissues are given in Table 17.4. This table can be summarized as follows:

Difference Between Results (%)	No. of Values
<10	13
10–20	10
20–40	7

The data on bone in Tables 17.3 and 17.5 can be summarized as follows:

Difference Between Results (%)	No. of Values
<10	7
10–20	15
20–40	1

These figures represent the combined errors of the two methods and include any sampling error that might be present. They indicate satisfactory accuracy of the Quantometer values.

Plans have been developed to provide the Quantometer with an automatic readout based on punched paper tape. This tape, containing calibration and sample data, will be processed by computer to yield elemental concentrations in the sample. The necessary components for building the tape punch attachment have been ordered, and the computer program for processing the tape is being written.

1147621

1147622

Table 17.4. Emission Spectrographic (Quantometer) and Atomic Absorption Values from Soft-Tissue Ash (μg per Gram of Ash)

Sample No.	Zn		Cd		Pb		Ni		Mn	
	Quantometer	At. Absorp.	Quantometer	At. Absorp.	Quantometer	At. Absorp.	Quantometer	At. Absorp.	Quantometer	At. Absorp.
YN-1 (kidney)	1700	1610	500	465			500	400	60	63
YN-2 (kidney)							350	320		
YN-3 (kidney)							220	240		
YN-4 (kidney)							160	150		
YN-7 (kidney)	7400	6240	1800	1380					68	73
276 K	3300	3770	1300	1290					82	112
307 K	3000	3440	1200	1280					110	142
312 K	2000	2990	600	790					90	124
323 K	4400	4920	4800	4850	80	100			88	110
307 L	5900	5550	140	132	150	120			240	207
324 L	5100	4520	220	212	180	150				

Methods have been considered for pulverizing large samples of wet tissue so that small representative samples can be obtained. Impact pulverization of the tissue at dry ice temperature appears to offer the best possibility. Other methods for grinding wet tissue involve metal-to-metal wear in the mill, which results in severe sample contamination. Test samples of beef muscle, fat, and bone were sent to the Pulverizing Machinery Company for trial processing in an impact mill. The samples were pulverized satisfactorily but showed contamination from the stainless steel mill that was used. A mill of this same type but made from hardened carbon steel has been ordered. This should reduce the sample contamination problem, but if it is still serious a special liner made from tungsten or some similar material will be made for the mill.

The analysis of bone for both trace and major constituents and of soft tissues for trace elements is being carried out on a routine basis. Flame spectrophotometry, colorimetry, and atomic absorption spectroscopy were used to test the accuracy of the Quantometer values. In each case the agreement was generally good.

Table 17.5. Emission Spectrographic and Atomic Absorption Values from Bone Ash (μg per Gram of Ash)

Sample No.	Zn		Sample No.	Mg	
	Quantometer	At. Absorp.		Quantometer	At. Absorp.
300 B	190	190	253 B	4700	4620
303 B	220	270	254 B	4600	4450
304 B	180	260	263 B-1	4100	4430
305 B	160	165	263 B-2	4300	4360
306 B	180	200	346 B	5300	5740
			352 B	3600	4260
			372 B	4200	4430
			376 B	4900	4620

1147623

19. Applied Internal Dosimetry

ORNL IN VIVO GAMMA-RAY SPECTROMETRY FACILITY

P. E. Brown
L. B. Farabee
G. R. Patterson, Jr.
J. L. Thompson
W. H. Wilkie, Jr.
L. S. Barden[1]
J. H. Dobkins[3]
B. A. Flores[2]
D. L. Mason[4]
S. L. Wood[5]

The ORNL in Vivo Gamma-Ray Spectrometer Facility, in operation since June 1960, has been applied primarily as a monitoring device to aid in the detection and measurement of internal exposures. As a result of instrumentation and program improvements made during the past year, it has been possible to increase the rate of routine counting for monitoring purposes and, at the same time, initiate a limited program of research. A computer program, which was being developed and tested during the early part of this report period, was designed to reduce the amount of facility time required for routine data processing and reporting. The program has been completed; however, several major revisions were required during the last few months in order to use the program on the new digital computer which was installed at ORNL in February and March 1963. The routine monitoring program, previously confined to examination of known or suspected exposure cases, has been expanded in scope. Increased emphasis is being placed on routine counting of potentially exposed persons and also on obtaining base-line counts for individuals prior to their entering new work involving potential internal exposure. During the past year, 492 human counts were made. The current rate of counting is about 110 persons per month, excluding instrumentation downtime. Table 19.1 summarizes the data for those cases in which measurable amounts of internal radioactive contamination were observed.

[1]ORINS undergraduate trainee, Hendrix College, Conway, Ark.

[2]Mathematics Division.

[3]Temporary summer employee, North Carolina State College, Raleigh, N.C.

[4]Temporary summer employee, Austin Peay State College, Clarksville, Tenn.

[5]ORINS research participant, Austin Peay State College, Clarksville, Tenn.

Table 19.1. Measurable Radioactivity Found in Routine Whole-Body Monitoring Program During the Period June 1, 1962, to May 31, 1963

Isotope	Number of People	Highest Quantity[a] Measured (μc)	Maximum Permissible[a] Burden (μc)
Cs^{137}	64	0.57	30
Na^{24}	1	0.14	7
I^{131}	19	0.28[b]	0.7[b]
Zr^{95}	21	0.014	20
Sb^{125}	4	0.006	40
Sr^{90}	2	0.04[c]	0.8[c]
Co^{60}	5	0.002	10
Zn^{65}	4	0.003	60

[a]Whole body, except as noted.
[b]Thyroid.
[c]Lung.

HUMAN UPTAKE AND EXCRETION OF I^{131}: ACCIDENTAL INHALATION AND CHRONIC AND SINGLE INGESTION OF IODINE IN MILK

G. R. Patterson, Jr.
G. W. Royster, Jr.
S. R. Bernard
L. B. Farabee
B. R. Fish
P. E. Brown

In the previous progress report,[6] Dowex 1-X8 resin was shown to be about 90% effective in removing I^{131} from cow's milk. The 10% I^{131} content lost to the column effluent milk was shown to be bound to protein. During the present report period, a study was undertaken to investigate whether or not the uptake and excretion of protein-bound I^{131} are significantly different from the uptake parameters utilized by the ICRP and NCRP[7] in estimating thyroid radiation dose and maximum permissible concentrations of I^{131}.

[6]L. B. Farabee, *Health Phys. Div. Ann. Progr. Rept. July 31, 1962*, ORNL-3347, pp 149–52.

[7]Report of Committee II on Permissible Dose for Internal Radiation (1959), *Health Phys.* 3 (1960); and *Natl. Bur. Std. (U.S.), Handbook 69* (1959).

1147624

The study was conducted in two separate phases. In the first phase, three male volunteers each day for 11 consecutive days ingested 150 $\mu\mu c$ of the protein-bound I^{131} contained in resin-treated milk. With the use of a 4- by 4-in. lead-collimated NaI(Tl) crystal, in vivo determinations indicated that the protein-bound I^{131} was taken up by the human thyroid.

The second phase of the study was undertaken in cooperation with the Internal Dose Estimation Section to obtain human data with which to evaluate the ICRP-NCRP parameters, assumptions, and predictions. In this phase, two of the volunteers who had participated in the first phase each ingested single intakes of 92 nanocuries of protein-bound I^{131} in milk. Three additional volunteers each ingested 1.84 nanocuries/day for 63, 8, and 4 consecutive days. As nearly as possible, the time interval between consecutive doses was maintained at 24 hr. Table 19.2 shows the age and weight of subjects, amount of ingested activity, estimated peak dose rate, and total dose received by the thyroid gland. All subjects were found to be euthyroid, as indicated by standard tests of protein-bound iodine in blood.

Thyroid counts were made using a 3- by 3-in. lead-collimated NaI(Tl) crystal connected to an RIDL 200-channel analyzer. Figure 19.1 shows a subject in the thyroid counting position.

Figure 19.2 presents the thyroid-gland data for the two subjects who ingested 92 nanocuries. Plotted on the ordinate is the percent of ingested dose present in the thyroid; on the abscissa is the time after ingestion. At first the buildup of I^{131} in the thyroid gland is very rapid, but it levels off at about four days, at which time the amount of I^{131} begins to decrease along a single exponential path. The data from the decay curve for I^{131} in the thyroid were treated by the method of least squares according to the equation

$$\phi = \sum_{i=0}^{n} W_i (Y_i - Y_{oi})^2 ,$$

where

ϕ = residual sum of squares,

Y_i = calculated ith value of the ordinate,

Y_{oi} = observed value,

W_i = weight factor.

The least-squares method was programmed for the IBM 7090 computer by George Atta of the Mathematics Division. Calculations were made using two sets of weight factors in which $W_i = 1$ (i.e., unit weight) and W_i^{-1} = var Y_i. Because it was assumed that all the variance in the ordinate value was due to counting, the variance was

Table 19.2. Data on Human Subjects Participating in the Protein-Bound I^{131} Experiment

Subject[a]	Age (yr)	Weight (lb)	Daily Intake ($\mu\mu c$/day)	Duration of I^{131} Ingestion (days)	Single Intake ($\mu\mu c$)	Maximum Dose Rate to Thyroid Gland (rem/week)	Total Dose to Thyroid (rem)
A	36	220	150	11	92,000	0.110	0.176
B	36	187	150	11	92,000	0.055	0.076
C	37	225	1840	63	0	0.005	0.056
D	53	170	1840	8	0	0.005	0.010
E	42	152	150 1840	11 4	0 0	0.005	0.015
Av	41	191					

[a]All subjects were euthyroid, as indicated by tests of protein-bound iodine in blood performed by the ORNL Health Division.

1147625

UNCLASSIFIED
PHOTO 61276

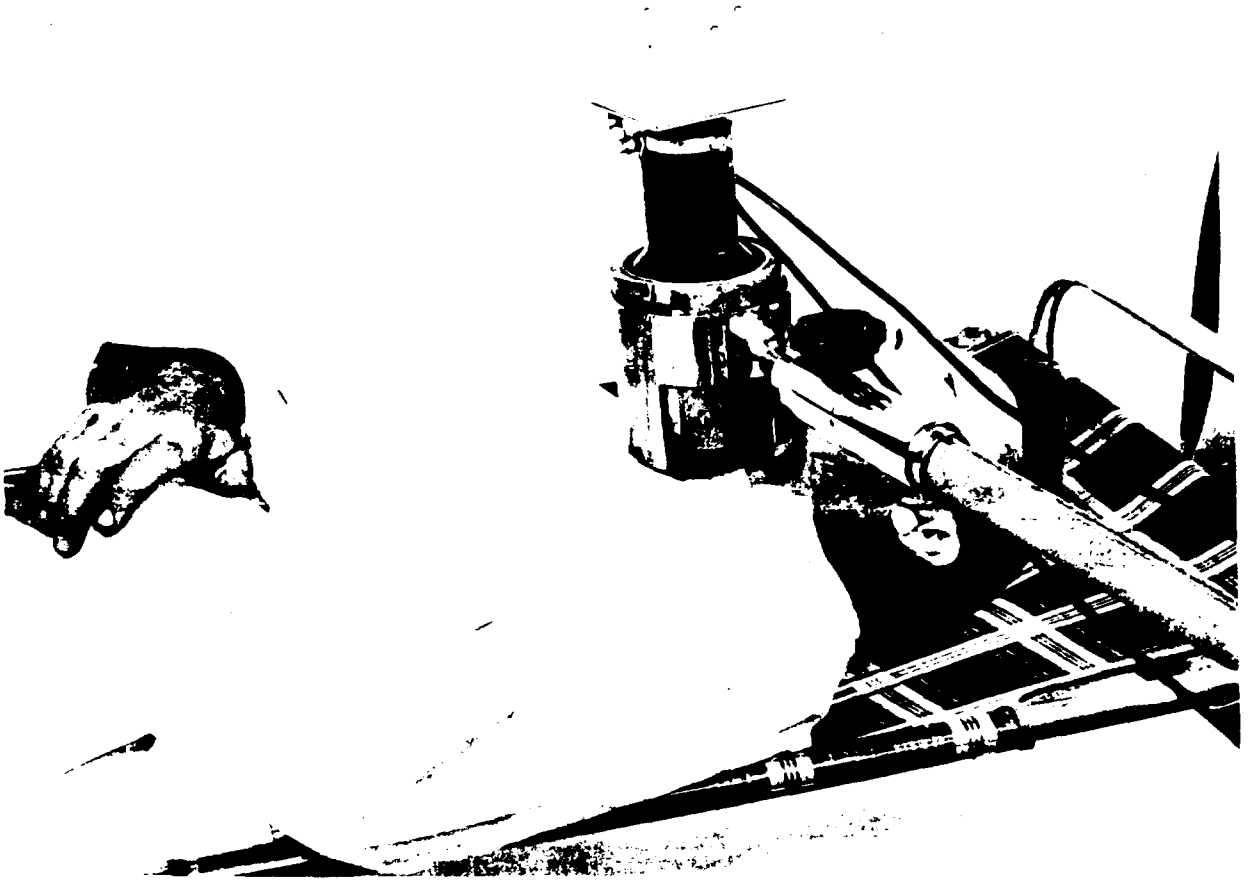

Fig. 19.1. Subject in Thyroid Counting Position.

estimated from the counts. The effect of weighting the residuals is to remove the bias of the smallest ordinate values (those containing the largest error) on the best-fitting curve. Figure 19.3 is a plot of the least-squares treatment of raw data for the two single-intake subjects. Figure 19.3*a* shows the data, together with the plot of the best-fitting curve for the case of $W_i = 1$ (i.e., unweighed data) and the equations for the curves. The errors on the parameters are two standard errors. On the ordinate are plotted the counts per minute in the thyroid gland, while on the abscissa is plotted the time in days.

Figure 19.3*b* is a plot of the data together with the best-fitting curves obtained when W_i^{-1} = var Y_i. Plotted along the ordinate are the counts per minute of the thyroid gland, while on the abscissa is the time in days following the single ingestion. Table 19.3 presents the rounded-off values of f_w and T_b for these two subjects. Using intercepts of the best-fitting curves and dividing by the amount ingested, estimates are obtained of f_w, the fraction going from the gut to the thyroid gland.

Although the f_w values (Table 19.3) for subjects A and B differ, the weighted and unweighted data have little influence on the f_w value for each individual subject. The biological half-lives T_b are quite different for subject A when the estimates are based on weighted and unweighted data. This is due to the fact that the effective decay constant λ approaches the radiological decay constant λ_r in the denominator of the equation

1147626

Table 19.3. Biological Values Estimated from Best-Fitting Parameters Obtained by Least-Squares Treatment of I^{131} Decay in Thyroid

Subject	Ingested Dose[a] (counts/min)	Fraction from GI Tract to Thyroid, f_w			Biological Half-Life, T_b (days)		
		Weighted	Unweighted	Weighted[b]	Weighted	Unweighted	Weighted[b]
A	10,090	0.28	0.27	0.29	291	1823	153
B	10,090	0.14	0.14		37	36	

[a]Based on 92 nanocuries at 4.94% thyroid counting efficiency.

[b]Last three measurements of curve for subject A omitted from least-squares calculation (see text).

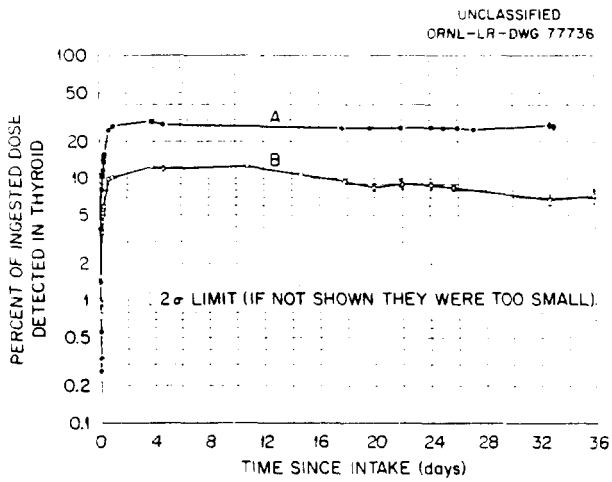

Fig. 19.2. Thyroid Gland Data for Two Subjects Who Ingested 92 Nanocuries of Protein-Bound I^{131} in Milk.

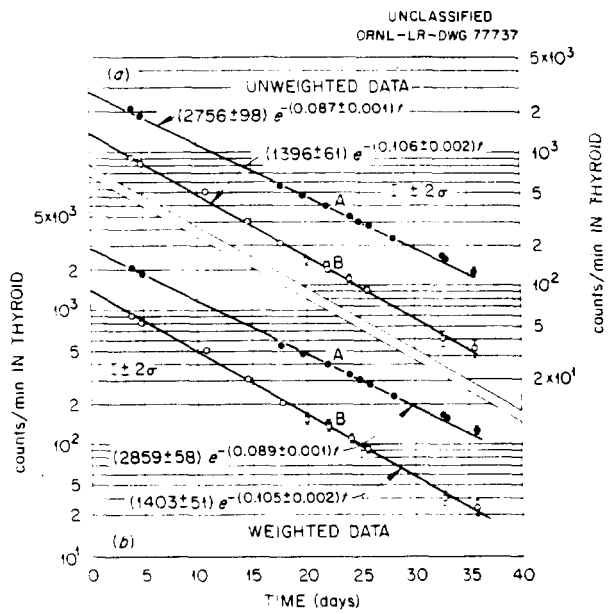

Fig. 19.3. Least-Squares Treatment of Thyroid Decay Curves.

for T_b [$= 0.693/(\lambda - \lambda_r)$], and T_b is quite sensitive to small changes in the denominator. The last three measurements for subject A markedly affect the value of λ and, hence, the calculated value of T_b. These last three points have larger variance than any of the other points. It was felt that these points might be biased because his intake of milk contained I^{131} from fallout. At the time of these measurements, the dietary milk in his community was increasing in its content of I^{131}. [illegible]

and their thyroid glands were counted. Figures 19.4–19.6 show the measured thyroid burdens of these subjects and the burden predicted by extrapolation of the single-intake data. Also shown for comparison is the predicted burden using ICRP-NCRP parameter values. On the ordinates of these figures are plotted the I^{131} ($\mu\mu$c) in the [illegible]

than the ICRP-NCRP-predicted burden; nevertheless, it is an overestimate also.

The thyroid gland measurements on subjects C, D, and E, who were counted both during the period of ingestion and after intake stopped, will be shown later in this report. First, the measurements of the thyroid gland burden after stopping the intake will be examined. Figure 19.7 presents the data for I^{131} in the thyroid of subject C, who ingested 63 daily intakes, and of subject D, who ingested 8 daily intakes. Figure 19.7*a* shows the graph of the data and the best-fitting curves together with the parameters of the best-fitting equations estimated from least-squares treatment of the unweighted data. Figure 19.7*b* shows the same data, but the best-fitting curves and parameters were estimated from the least-squares treatment of weighted data. As can be seen in Fig. 19.7 the influence of the smallest ordinate value (the last point) is reduced when the weighted sum of squares is used. From these best-fitting equations, the values for the parameters f_w and T_b can be obtained for these two subjects, and the iodine burdens in the thyroid glands during the period of chronic intake can be predicted and compared with the measured burdens.

Table 19.4 presents the values for f_w and T_b obtained from the numerical data appearing in Fig. 19.7. For subject C the f_w value is quite different, depending on whether the weights were set equal to unity or to $1/(\text{var } Y_i)$. The same is true for the T_b for subject C. The parameters

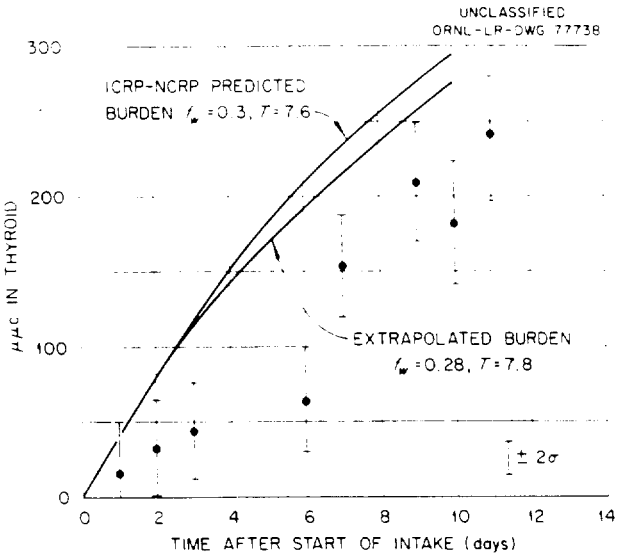

Fig. 19.4. Thyroid Gland Burden of I^{131}. Subject A ingested 150 μμc daily for 11 days in resin-treated milk.

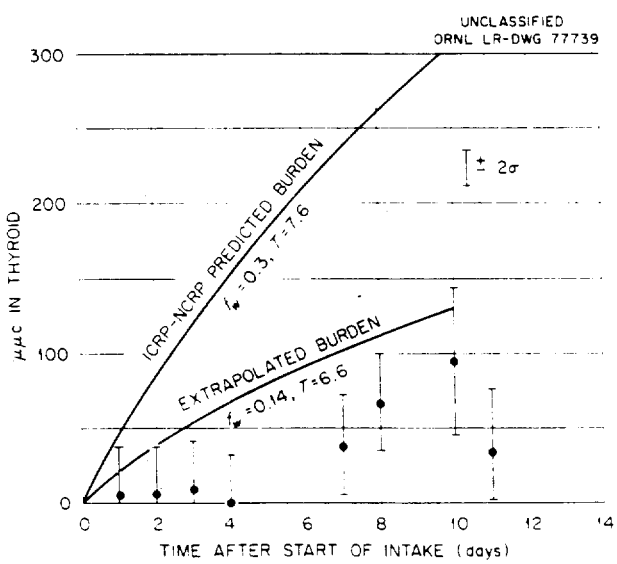

Fig. 19.5. Thyroid Gland Burden of I^{131}. Subject B ingested 150 μμc daily for 11 days in resin-treated milk.

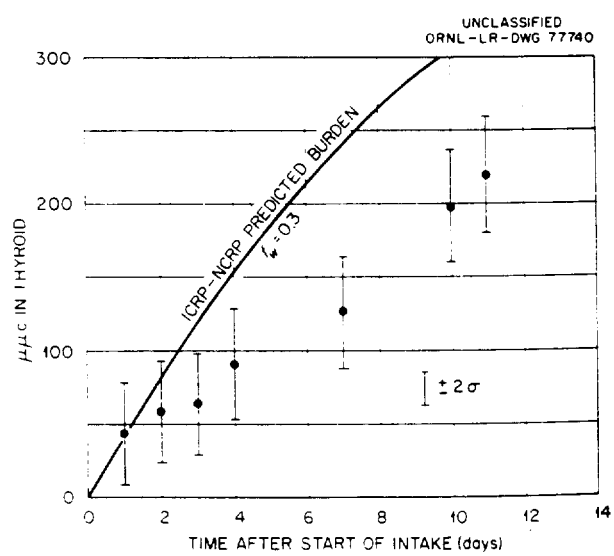

Fig. 19.6. Thyroid Gland Burden of I^{131}. Subject E ingested 150 μμc daily for 11 days in resin-treated milk.

1147628

obtained from the weighted least-squares treatment are employed to predict the thyroid uptake of I^{131} during daily ingestion.

Figures 19.8 and 19.9 show the thyroid burden measurements on these two subjects both during their period of daily intake and in the following period after the intake was stopped. Plotted on the ordinate is the I^{131} ($\mu\mu c$) in the thyroid, while plotted on the abscissa is the time in days from the first intake. Also shown in these figures are the predicted thyroid burdens employing ICRP-NCRP data and the extrapolated thyroid burdens based on the f_w and T_b values appearing in Table 19.4 (weighted data). For both subjects the ICRP-NCRP-predicted burdens overestimate the observed burdens. Also, in the case of subject C, the extrapolated burden from single-intake data slightly overestimates the observed level in thyroid.

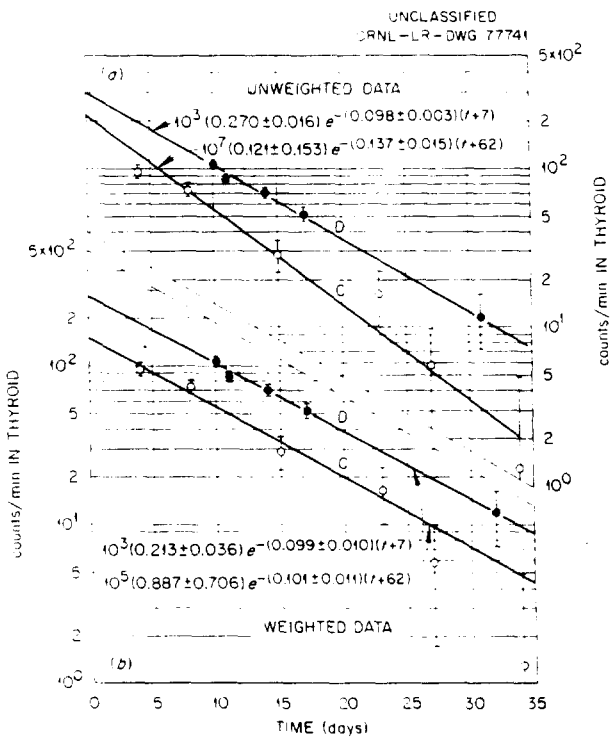

Fig. 19.7. Least-Squares Treatment of Thyroid Decay Curves.

Subjects A and B submitted urine samples for the first five days following their single ingestions; subject C submitted urine samples during the entire 63 days of continuous intake and 4 days following the end of intake. The samples constituted essentially total voiding during the above periods. An average of (64 ± 5)% of the ingested dose was excreted in urine during the first day after a single intake. In the continuous-intake case, the daily urinary excretion increased to about 95%/day when equilibrium was apparently reached.

The urinary excretion of I^{131} for subject C is shown in Fig. 19.10. Plotted on the ordinate is the percent of daily intake of I^{131}. The time in days after the first intake is plotted on the abscissa. During the first ten days, the measured excretion rate rises from 75%/day to a level of about 90 to 95%/day and from then fluctuates around 95%/day. Note that the point at 60 days is ~15%/day. On this day the subject had influenza, accompanied by diarrhea and vomiting. His urinary volume on this and the succeeding two days was quite low since he was on a negative water balance. It can be noted also that the rate of I^{131} excretion on these days was lower than usual. After the intake was stopped, the rate of excretion decreased precipitously. On the 66th day, three days after the ingestion of I^{131} had been stopped,

Table 19.4. Biological Values Estimated from Best-Fitting Parameters Obtained by Least-Squares Treatment of Thyroid-Decay-Curve Data

Subject	Daily Dose[a] (counts/min)	Fraction from GI Tract to Thyroid, f_w		Biological Half-Life, T_b (days)	
		Weighted	Unweighted	Weighted	Unweighted
C	202	0.08	0.17	47	14
D	202	0.14	0.14	57	61

[a]Based on 1.84 nanocuries per day at 4.94% thyroid counting efficiency.

1147629

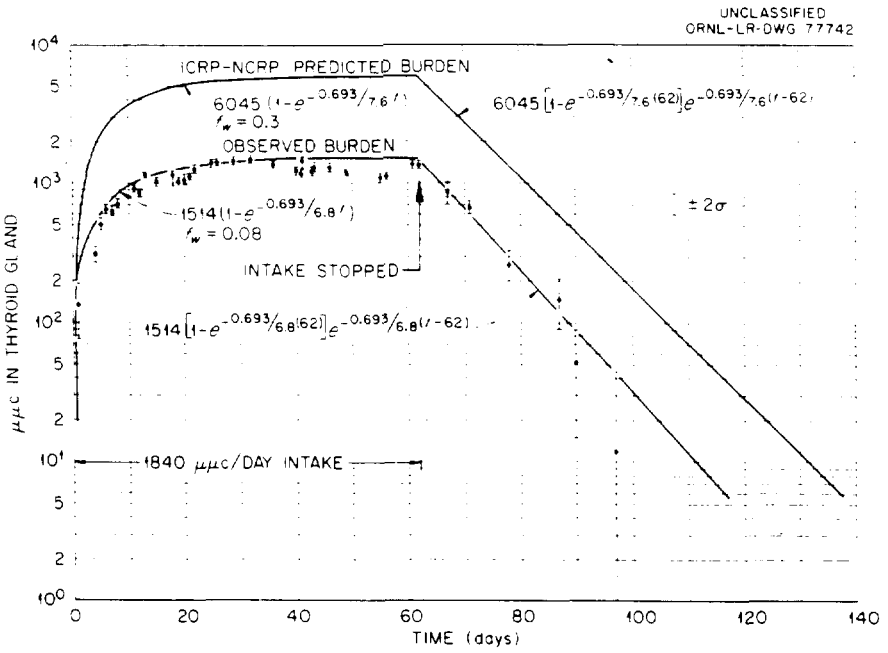

Fig. 19.8. Thyroid Gland Burden of I^{131}. Subject C ingested 1840 μμc daily for 63 days.

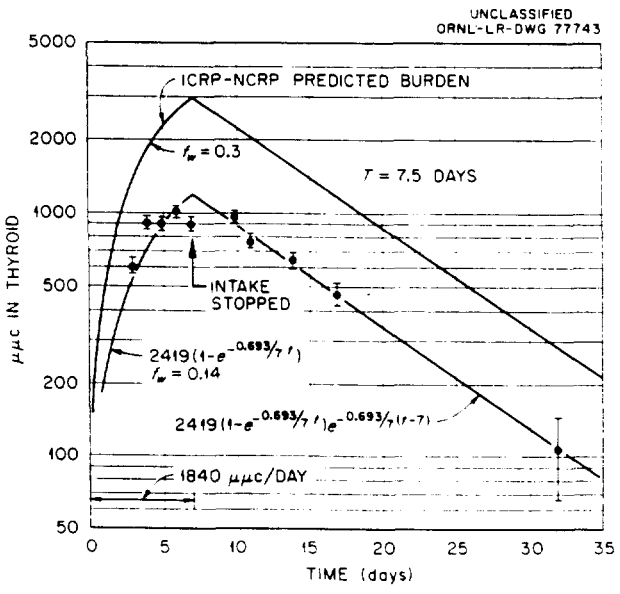

Fig. 19.9. Thyroid Gland Burden of I^{131}. Subject D ingested 1840 μμc daily for 8 days.

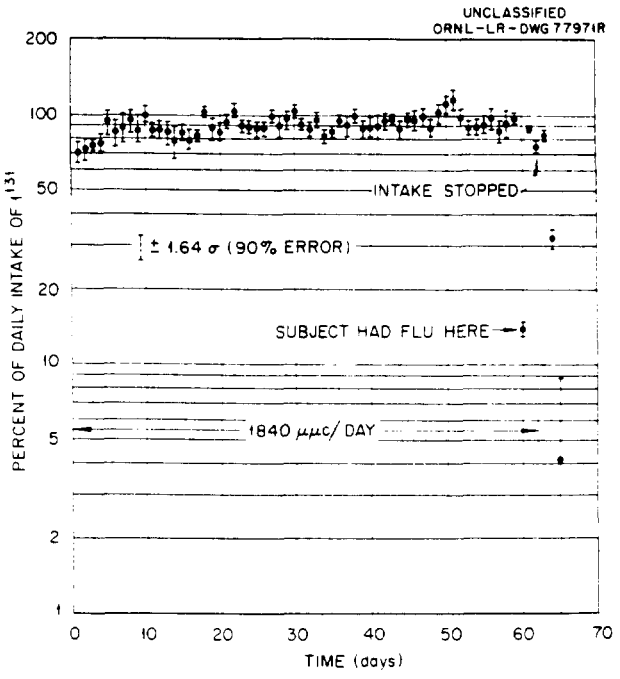

Fig. 19.10. Daily Urinary Excretion of I^{131}. Subject C ingested 1840 μμc daily in resin-treated milk for 63 days.

1147630

the level in urine was less than the limit of sensitivity for detecting I^{131} in urine.

Coincidentally, just before the second phase of the study began, an ORNL employee inhaled a small quantity of I^{131} vapor when a sample which was being poured out reacted with the slightly acid waste in the hot-sink drain trap. The employee was first counted for I^{131} thyroid activity 4 hr after the exposure incident; during the next 42 days, he was counted seven times for I^{131} thyroid activity and seven times to determine the whole-body burden. Figure 19.11 shows the spectrum from a typical thyroid count with the 3- by 3-in. crystal positioned over the employee's thyroid gland and in contact with his throat.

Figure 19.12 compares the decrease in thyroid burden for the inhalation case with the burdens for the two ingestion volunteers for the first 18 days following intake. The data points were not corrected for radiological decay; consequently, they are compared with the rate of elimination from the thyroid predicted by the ICRP-NCRP, $T_{eff} = 7.6$ days.[7]

The urinary excretion pattern of the inhalation case shows rather good agreement with excretion patterns for the two ingestion cases. The employee exposed by inhalation submitted essentially his total voiding for the first four days following exposure, beginning approximately 30 min after exposure. The two ingestion volunteers submitted essentially their total voiding during the same period. Figure 19.13 shows the comparison of urinary excretion for the three cases. Urine sample counts were corrected for radiological decay back to the time of intake in order to provide cumulative excretion data.

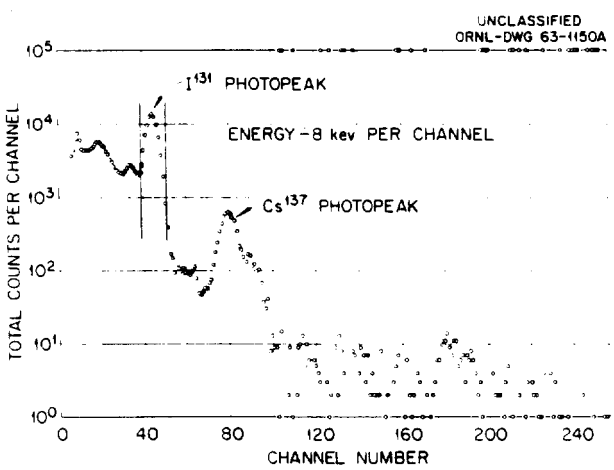

Fig. 19.11. Typical I^{131} Gamma-Ray Spectrum of 3- by 3-in. Lead-Collimated NaI(Tl) Crystal Positioned over Thyroid Gland.

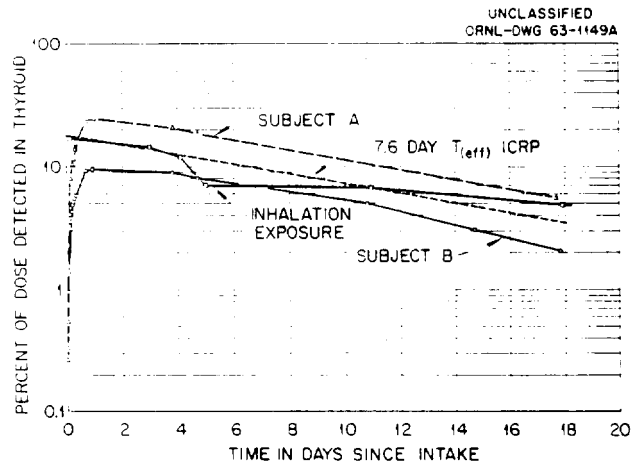

Fig. 19.12. Percent of Initial I^{131} Intake Found in Human Thyroid. Comparison of two cases of single oral ingestion (A and B: 0.092, in milk) with one case of single inhalation of I^{131} vapor (estimated 0.740 μc, WBB).

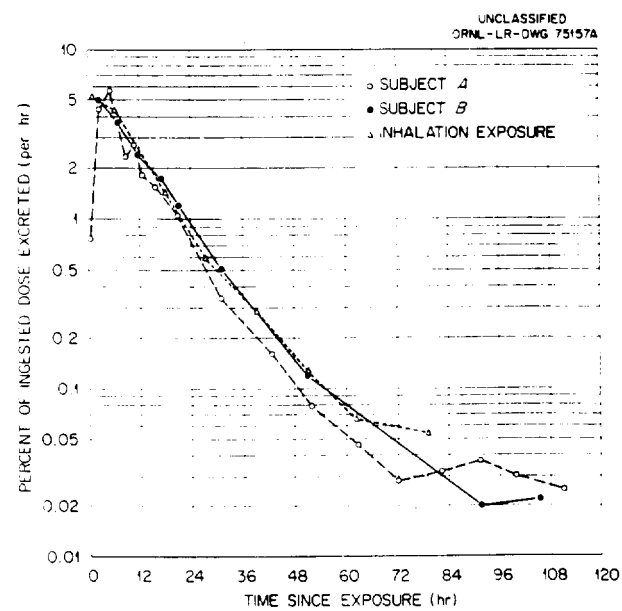

Fig. 19.13. Comparison of Urinary Excretion for Three Cases.

1147631

From Figs. 19.12 and 19.13, it is seen that subject A had a higher thyroid uptake and lower excretion; subject B had a high excretion and lower thyroid uptake. Although two subjects do not constitute a good statistical sample, these two apparently provide a reasonably good average excretion factor. Keating *et al.*[8] found the average cumulative excretion for apparently normal thyriod cases to be approximately 64.5% of the dose at the end of 48 hr; the average for the two volunteer subjects was approximately 65% of the ingested dose excreted by 48 hr.

The patterns for thyroid uptake and urinary excretion of radioiodine appear to be strikingly similar, whether the dose is acquired by inhalation or ingestion. Since this seems to be true, the data obtained from the I^{131} ingestion study were useful in estimating the extent of the inhalation exposure. Based on the ingestion data, the initial inhalation exposure was estimated to have been approximately 740 nanocuries in the whole body. Extrapolating thyroid counts for the inhalation case back to time of intake gives approximately 135 nanocuries in the thyroid. This is approximately 18% of the whole-body burden.

For the sake of comparison, had the exposure been sustained at the original level, it would be approximately 96% of the MPC for continuous exposure (ICRP-NCRP).[7] It is more nearly correct, however, to compare this single acute inhalation with the maximum permissible quarterly intake by inhalation (ICRP-NCRP, 4.4 μc), in which case this exposure amounted to approximately 16.8% of the permissible quarterly intake.

In conclusion, the present study suggests that the single-intake data can be extrapolated to the case of continuous intake when the parameters are estimated for each individual. It is also suggested that the single-exponential-compartment model of ICRP-NCRP is a fairly adequate representation of the data on I^{131} uptake by human thyroid glands. It is to be remembered that the foregoing statements are only suggestions, and they rest on relatively few cases observed over periods of time that are short compared with a 50-yr-exposure period. It is indicated from these few human studies that the ICRP-NCRP recommendations of $(MPC)_w$ are conservative and differ by a factor of only ~ 2.

[8] F. R. Keating *et al.*, *J. Clin. Endocrinol.* 10, 1425 (1950).

COMPUTER PROGRAM FOR IN VIVO COUNTING DATA

G. R. Patterson, Jr. B. A. Flores

Program WBC is designed to process data from the RIDL 200-channel analyzer and the Nuclear Data 512-channel analyzer. Data in the form of punched paper tape are transferred to magnetic tape on the CDC 160-A computer and are merged on the CDC 1604 computer with other information concerning the in vivo count. The 1604 program processes the individual spectra according to the indicated counting geometry and stores the original spectrum, coded information, net spectrum, and output information on magnetic tape for future use.

The code strips K^{40} and Cs^{137} from the net spectrum and calculates two estimates of the grams of total potassium according to the summation of counts both in the photopeak and in the Compton scatter band, the nanocuries of Cs^{137}, and the standard deviations of these estimates. A plotting subroutine prepares instructions on magnetic tape, which is used with a Calcomp plotter to graph the net spectrum and the net spectrum minus K^{40} and Cs^{137}. This subroutine can be instructed to sum two or more adjacent channels and plot as a single data point, permitting a rudimentary form of curve smoothing.

Figure 19.14*a* shows a portion of the computer printout for a routine in vivo count of an ORNL employee. The personal information identifying the count was supplied to the computer from in vivo count data sheets. Figure 19.14*b* shows the Calcomp plot of the spectrum for the same employee. Each point shown is the sum of two adjacent channels plotted at the "midpoint" position. Note the net spectrum, showing peaks for K^{40} around channel 180, Cs^{137} around channel 81, and I^{131} around channel 45. In the second curve (net spectrum minus K^{40} and Cs^{137}), the potassium and cesium peaks have been stripped out, but the I^{131} peak is still very much in evidence, reduced only slightly by the stripping of the potassium and cesium contribution.

The program originally was written for the IBM 7090 to be processed at Central Data Processing, ORGDP. In this format, the program was almost ready for use in December 1962, but changes in computer equipment, both at Central Data Processing and at ORNL, necessitated a major program

1147632

UNCLASSIFIED
ORNL-DWG 63-2423

PART A

NAME BADGE DEPT. BLDG. DATE 3-22-63 TENN SPEC. TIME

RUN NO. COUNT TIME (MIN.) 20 GROSS INT. CT. 91943 GROSS CT. (M.E.A.) 2718

MONITOR INT. CT. CHEST CIRC. IN WAIST IN

BODY D SEX PREVIOUS NO. 0

		CS137	K40-SCATTER	K40-PHOTO	TOTAL	HI
BANDS						
SUMS(C/M)	524.72	78.34	44.25	92.00	3449.45	530.55
SUM/KG	4.8	.73	.41	.80	23.70	5.15
STD. DEV.						
NET						
NET-K40						
NET-K40-CS						
ESTIMATES			23.2984 GRAMS	44.0776 GRAMS		
STD. DEV. %						
ESTIMATES						

NET SPECTRUM

38.50			27.50	35.40	43.05	53.05	56.45	62.00	52.35
63.30	66.75	65.45	66.15	66.35	65.05				
62.45	64.15	60.15							

PART B

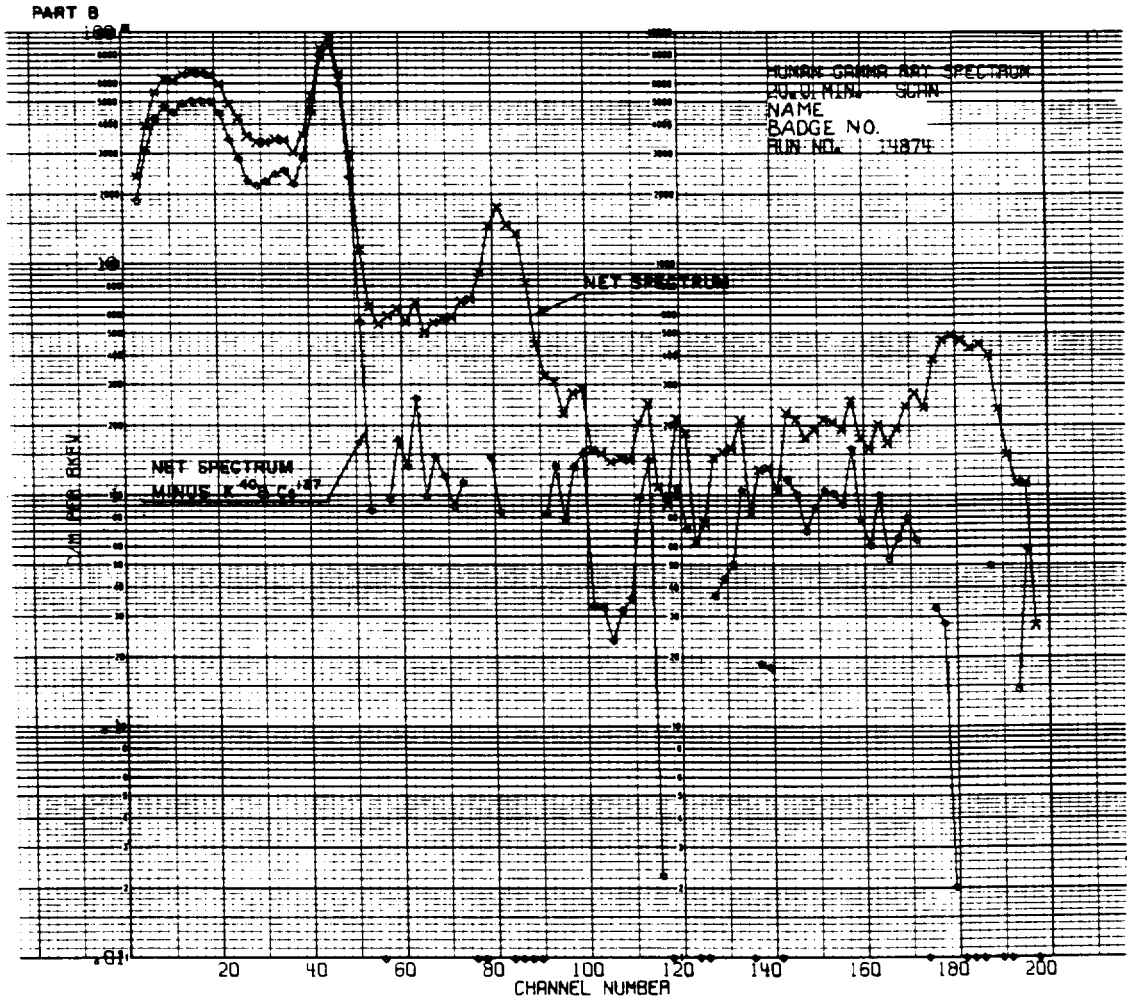

Fig. 19.14. In Vivo Data Printout.

1147633

rewrite. The CDC 160-A, on which punched paper tapes were transferred to magnetic tape, was moved from Central Data Processing to the High Voltage Laboratory at ORNL and was replaced with an IBM 1401. The 1401 could not handle the WBC program input without a major program rewrite, and the 160-A in its new location at ORNL had been modified so that it no longer could handle the WBC program input. The decision was made to rewrite the program to utilize the new CDC 160-A and 1604 complex which was being installed at ORNL to replace the Oracle. This rewrite has been accomplished and is being debugged. At the present time the program seems to be capable of handling the data for routine in vivo counts and of providing satisfactory estimates of total K and Cs^{137}.

DEVELOPMENTS IN THE ORNL IN VIVO GAMMA-RAY SPECTROMETRY FACILITY

W. H. Wilkie, Jr.

During the past year several improvements have been made in the IVGS Facility. All routine human in vivo counts are now made in a scanning bed geometry in which an individual lying horizontally on a bed is moved beneath a NaI(Tl) crystal. At the same time that the gamma spectrum is being analyzed, a strip-chart recorder traces the gross counting rate as a function of detector position along the body. The scanning bed replaces the chair geometry formerly used in our routine program. Although a thorough study has not yet been completed, it is estimated that the efficiency for gamma detection using the scanning bed geometry is approximately equal to that of the chair geometry for radionuclides uniformly distributed in the body and is less sensitive to changes in geometry resulting from nonuniformly distributed radionuclides or from variations in size between individuals.

A thin-crystal assembly is now available for use in the spectral analysis of electromagnetic radiation in the energy region below 150 kev. The assembly consists of three 5-in.-diam by $^1/_{16}$-in.-thick NaI(Tl) crystals with a 5-mil beryllium entrance window and mounted on 5-in. photomultiplier tubes. Signals from these three tubes are linearly mixed, amplified, and sorted in a multichannel pulse-height analyzer. A normal human spectrum obtained with the thin-crystal assembly is composed of counts due to the K^{40} and Ba^{137} gamma rays, a Ba^{137} x ray, and a residual gamma flux. Figure 19.15 shows a typical thin-crystal-assembly spectrum of the residual portion of a human chest count (average of seven unexposed males); that is, the spectrum with the contributions from K^{40} and Ba^{137} removed. The origin of the residual spectrum has not been adequately explained and is being studied further.

The thin-crystal spectrum of an individual containing a small amount of Sb^{125} is shown in Fig. 19.16. The amount was determined to be less than 10^{-4} times the maximum permissible body

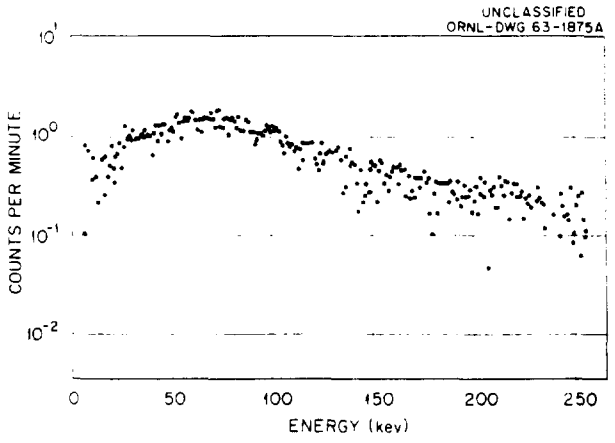

Fig. 19.15. Typical Thin-Crystal-Assembly Spectrum of a Residual Portion of a Human Chest Count.

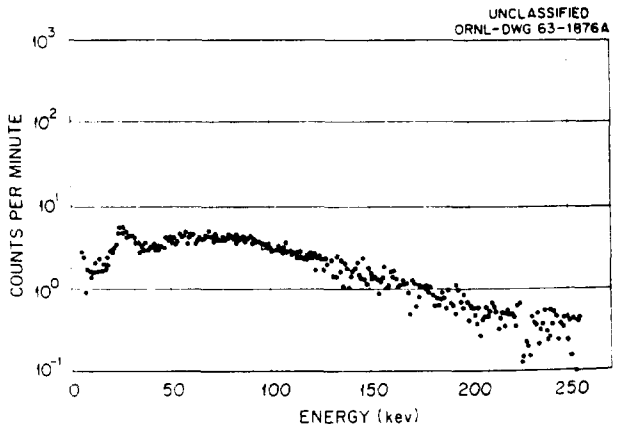

Fig. 19.16. Thin-Crystal-Assembly Spectrum of an Individual Containing a Small Amount of Sb^{125}.

1147634

burden (MPBB).[9] The thin-crystal assembly is of particular importance in the study of lung burdens of plutonium. In its present state of development the assembly is capable of detecting less than 40 nanocuries of Pu^{238} in the human lung in a 40-min chest count, provided that a background is available on the individual prior to the Pu^{238} inhalation. If no prior background is available, the Pu^{238} burden detectable is 80 nanocuries or less. Figure 19.17 shows a typical calibration spectrum for Pu^{238} in the lung. The lowest-energy peak is due to the 17-kev x-ray group of uranium.

An attempt was made to reduce the background in the iron room by installing a graded shield over the existing ⅛-in. lead lining of the room. A layer of tin and cadmium approximately 0.04 in. thick was laid on top of the lead on the floor, a layer of copper 0.01 in. thick was placed over the tin and cadmium, and the original vinyl tile was then replaced. On the basis of similar background counts, using the 8- by 4-in. NaI(Tl) crystal before and after the operation described, it was concluded that the background below 2 Mev had been reduced by 24%. Further developments include the installation of the thin-crystal assembly adjacent to the large NaI(Tl) crystal, permitting their use concurrently.

[9]Report of Committee II on Permissible Dose for Internal Radiation (1959), *Health Phys.* 3 (1960).

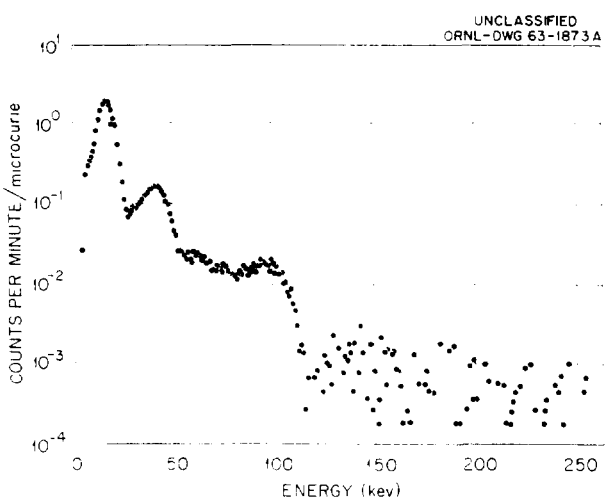

Fig. 19.17. Typical Calibration Spectrum for Pu^{238} in the Lung.

METHOD FOR REMOVAL OF ALPHA CONTAMINANTS IN PHOSPHORIC ACID

L. B. Farabee

Gross alpha transuranic radionuclides in a urine sample are determined most expediently by a cursory method which concentrates the total alpha activity by a bismuth phosphate–lanthanum fluoride precipitation ($BiPO_4$-LaF_3). This procedure isolates as a group the isotopes of Th, Np, Pu, Am, Cm, Bk, and Cf. Since the urinary alpha radioactivity excretion rates of these radionuclides associated with a maximum permissible exposure are very low, the chemical reagents used in the isolation procedure must be free of extraneous alpha activity in order that the background be held to a minimum. The elimination of alpha-active impurities from lanthanum has been described.[10] This study is concerned with identification of alpha-radioactive impurities in phosphoric acid (H_3PO_4) and a method for their removal.

Although phosphates are normal constituents of urine, excess phosphate (as H_3PO_4) is added to ensure complete precipitation of the bismuth "carrier" in the $BiPO_4$ procedure. In one procedure for isolating plutonium from a 1500-ml urine sample by $BiPO_4$ precipitation,[11] the 10 ml of added H_3PO_4 increased the alpha background by 0.4 dis/min. Radium D (Pb^{210}) and its daughters were found in this H_3PO_4, and the alpha of Po^{210} is no doubt the cause of the increased background counts in the reagent blank.

The radioactive contaminants in H_3PO_4 are so low that concentration of these radionuclides on a cation exchange resin column is necessary before identification can be made. The presence of Pb^{210} and Bi^{210} in H_3PO_4 was proved by a procedure of Baratta and Herrington,[12] while Po^{210} was determined by a plating technique.[13] Decay and/or growth studies confirmed the presence of Pb^{210} and Bi^{210}. Radium D and its daughters were found in samples from five different sources

[10]L. B. Farabee, *The Removal of Alpha Contamination from Lanthanum by Ion Exchange*, TID-7591, pp 78–80 (Oct. 1–2, 1959).

[11]L. B. Farabee, *Procedure for the Determination of Plutonium in Human Urine*, MonH-218 (April 1947).

[12]E. J. Baratta and A. C. Herrington, *The Determination of Isotopic Radium*, WIN-118 (September 1960).

[13]E. S. Spoerl, *Urine Assay Procedure at the Mound Laboratory*, AECD-3811 (April 1950).

1147635

of H_3PO_4. The Po^{210} alpha activity ranged from 70 to 1330 dis min^{-1} $liter^{-1}$. The H_3PO_4 was also analyzed for Ra^{226}; however, the Ra^{226} contribution was seen to be less than 1 part in 500 of the Po^{210} alpha activity of the reagent. Apparently Ra^{226} is removed in the process of preparing H_3PO_4.

Quantitative removal of the contaminants is achieved by passing a 2 *M* H_3PO_4 solution through a cation exchange resin column (35 ml of Dowex 50-X12 (−50 + 100 mesh) in a 1.8-cm-ID cylindrical glass column) at a flow rate of 3.8 ml cm^{-2} min^{-1}. This purification will reduce the alpha background of H_3PO_4 from about 0.4 to <0.08 dis/min per sample.

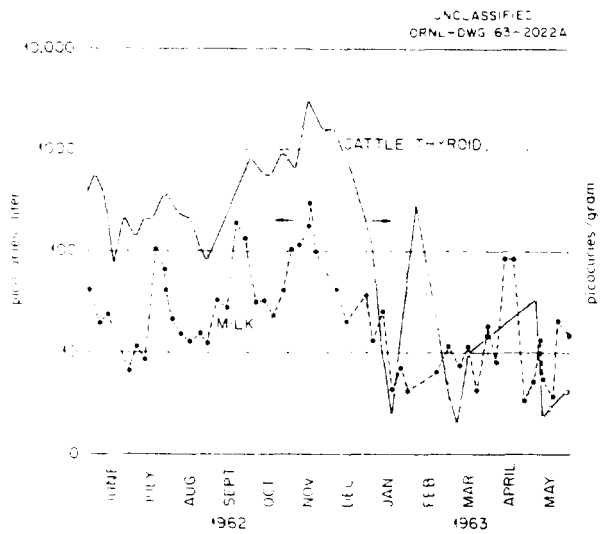

Fig. 19.18. Iodine-131 in Cattle Thyroids and in Milk in the East Tennessee Area.

IODINE-131 IN MILK AND IN CATTLE THYROIDS

J. L. Thompson B. R. Fish

During the period June 1, 1962, to May 31, 1963, a total of 285 cattle thyroids and 70 milk samples have been analyzed for I^{131}. It has been observed that the I^{131} concentration can differ by a factor of 3 or more in thyroids from cattle on the same farm and in milk from cows on the same farm. Thus, it is important to collect a fairly large number of samples from a given region in order to get a reasonable average for the concentration of I^{131} in milk. During the period of highest I^{131} levels, through December (Fig. 19.18), a larger number of samples were collected on each date; therefore, these data are considered to be more representative of the average I^{131} levels than the results of spot sampling in the later five months. These data suggest that the average concentration of I^{131} per liter in milk is about 8% of the average concentration per gram in cattle thyroids.

The I^{131} content in 280 liters of milk is approximately equal to the total I^{131} in one thyroid of cattle (average weight of thyroid, 22.4 g). For equal detection sensitivities the milk must be reduced about 8000 to 1 in volume. These facts emphasize the utility of including cattle thyroid sampling in a program for the monitoring of I^{131} in the environment. In addition to the milk sampling program the cattle thyroid monitoring program is suggested as another biological monitor which provides an extremely sensitive detection limit but requires a minimum amount of laboratory preparation.

1147636